Fermi-liquid theory of imbalanced quark matter

J. J. R. M. van Heugten, Shaoyu Yin,* and H. T. C. Stoof

Institute for Theoretical Physics, Utrecht University, Leuvenlaan 4, 3584 CE Utrecht, The Netherlands

The temperature dependence of the thermodynamic potential of quantum chromodynamics (QCD), the specific heat, and the quark effective mass are calculated for imbalanced quark matter in the limit of a large number of quark flavors (large-N_F), which corresponds to the random-phase approximation. Also a generalization of the relativistic Landau effective-mass relation in the imbalanced case is given, which is then applied to this thermodynamic potential.

I. INTRODUCTION

Landau Fermi-liquid theory has seen considerable success in describing a wide variety of fermionic many-particle systems, such as liquid Helium-3, electrons in metals, nuclei and nuclear matter [1–4]. It gives an effective description of the low-lying elementary excitations (quasiparticles) at low temperatures, i.e., at a temperature T such that the system can be considered degenerate ($T \ll \mu$, where μ denotes the chemical potential) but still in the normal phase above any symmetry breaking phase transition ($T \gg T_c$), for example, to a magnetic or superconducting phase. Nevertheless, the theory is not only important for the description of the above "normal" (Fermi-liquid) phase, but is also vital to correctly describe the emergence of a possible ordered phase [5]. Indeed, according to the Bardeen-Cooper-Schrieffer (BCS) theory the onset of superconductivity is to be viewed as an instability of the Fermi liquid under an attractive interaction, which results in the formation of Cooper pairs [6]. The same is true for magnetism in the case of repulsive interactions.

In particular, BCS theory implies that the high-density and low-temperature region of the phase diagram of quantum chromodynamics (QCD) contains a color superconducting phase of quarks [7,8]. In fact, since quarks carry color, flavor and spin quantum numbers, many distinct superconducting phases are possible and are characterized by the various symmetries of the Cooper-pair wave function. These phases of cold and dense QCD might occur in the core of neutron stars where matter is compressed to several times the nuclear density $\rho_0 \simeq 0.16$ fm^{-3}. The presence of such a superconducting phase is expected to have observable consequences on the cooling and magnetic fields of neutron stars [9–11].

Strictly speaking, Landau Fermi-liquid theory is valid in the normal phase, where the low-temperature properties of the system can be described in terms of a gas of weakly interacting, but possibly strongly renormalized, fermionic quasiparticles. Nevertheless, it is well known from superfluid Helium-3 that knowledge of the details of these quasiparticles is necessary to correctly describe the onset of superfluidity [12]. In color superconductivity, which is of interest to us here, we expect that the critical temperatures of the various color superconducting phases will also be affected by Fermi-liquid effects, which will modify the competition between these phases. A particularly interesting phase in this respect is the so-called 2SC phase in which only two flavors of quarks are paired, while the unpaired quarks of the third flavor remain a Fermi-liquid. This phase further illustrates the importance of understanding the quark-gluon plasma, i.e., the normal phase of quarks.

Fortunately, due to asymptotic freedom, the coupling constant g of QCD becomes small at large chemical potential μ, such that a systematic study of the high-density and low-temperature region of the QCD phase diagram is possible using perturbation theory. At high densities the dominant interaction between quarks is that of one-gluon exchange, where the long-range behavior of the gluons is screened due to the quark-gluon plasma. While the electric gluons (longitudinal) are screened by a Debye mass $m_g \sim g\mu$, the magnetic (transverse) gluons are only dynamically screened [13,14]. This residual long-range behavior of the magnetic gluons dominates the low-temperature behavior of the system. Examples of the effects of magnetic gluons can be seen in the nonstandard scaling of the critical temperature of the superconducting phase $T_c \sim \mu g^{-5} \exp(-3\pi^2/g)$ [15–17], which depends exponentially only on $1/g$ instead of showing the expected $1/g^2$ behavior, or of the lifetime of elementary excitations of (grand-canonical) energy E near the Fermi surface $\tau(E) \sim |E|^{-1}$ [18–21] that signals a (marginal) non-Fermi-liquid behavior at zero temperature.

In the context of a possible deconfined phase of quarks inside neutron stars, the Fermi system is expected to be imbalanced due to the different chemical potentials of the various quarks. This deconfined phase may contain u, d, and s quarks with different densities as a consequence of their different masses and charges. In cold atomic physics, an analogous population imbalance has been realized experimentally between two spin states [22,23], which

---

*s.yin@uu.nl

resulted in frustration of the pairing between particles. This will cause very different behavior from the normal BCS case and is currently a very hot topic in a wide variety of fields [24,25]. In particular, the imbalance between different flavors of quarks is expected to significantly alter the properties of the QCD phase diagram, such as the 2SC phase mentioned above or the color-flavor locked phase where all the colors and flavors are paired [7]. In the present paper, we therefore generalize the quasiparticle properties based on Fermi-liquid theory to an imbalanced system.

To do so, the effect of the dressed gluons on the thermodynamic potential, specific heat and effective mass of the quasiparticles is determined at low temperatures. The thermodynamic potential will be calculated for a two-flavor quark system in the limit of a large number of quark flavors (large-N_F). This approximation corresponds to the random phase approximation (RPA), which has been quite successful in condensed-matter systems such as the interacting electron gas in metals [26]. Using the framework of Landau Fermi-liquid theory for relativistic systems, derived in Sec. II, the effective mass of the quasiparticles can be determined from the thermodynamic potential by considering the specific heat. The result and its implications on the applicability of Fermi-liquid theory is discussed. As we will show, the logarithmic dependence of the temperature, which is due to the transverse gluons, shows the breakdown of Fermi-liquid theory at low temperatures. Furthermore, even though within our approximations there is no interaction between the different flavors of quarks in the limit of weak coupling, the RPA correction still presents some mixing between the different flavors, which stems from the long-wavelength screening of the longitudinal gluons. Above and throughout the article natural units are used, i.e., units such that $\hbar = c = k_B = 1$. Other conventions and technical details of the calculation can be found in the Appendices.

II. LANDAU FERMI-LIQUID THEORY

To describe the normal state of the quark-gluon plasma at nonzero temperatures, which is a strongly interacting gas of quarks, Landau Fermi-liquid theory can be used. This theory takes as a starting point the noninteracting Fermi gas and switches on the interaction adiabatically. As long as the temperature of the system is much higher than the critical temperature T_c for superconductivity, no bound states (Cooper pairs) will form and each state of the noninteracting Fermi gas is transformed into a state of the interacting gas. Therefore, the excitations of such a Fermi liquid remain of a fermionic nature. For simplicity, Fermi-liquid theory will be introduced here for a system at zero temperature even though the quark-gluon plasma is formally a marginal Fermi liquid in that case. However, the introduced concepts turn out to be valid for nonzero temperatures much lower than the Fermi temperature T_F,

which is expected to be around 10^{13} K for quarks in the core of neutron stars.

The basis of Landau Fermi-liquid theory is to consider the effect of a small change of the ground-state Fermi distribution on the thermodynamic potential density, which can be written as

$$\delta\Omega = -\sum_\sigma n_\sigma \delta\mu_\sigma + \frac{1}{V}\sum_{\mathbf{k},\sigma}(\epsilon_\sigma(\mathbf{k}) - \mu_\sigma)\delta N_\sigma(\mathbf{k})$$
$$+ \frac{1}{2V^2}\sum_{\mathbf{k},\sigma;\mathbf{k}',\sigma'} f_{\sigma\sigma'}(\mathbf{k},\mathbf{k}')\delta N_\sigma(\mathbf{k})\delta N_{\sigma'}(\mathbf{k}'). \quad (1)$$

Here, $\delta N_\sigma(\mathbf{k})$ is a small change in the ground-state momentum distribution of species σ, n_σ is the particle density, $\epsilon_\sigma(\mathbf{k})$ is the energy of a quasiparticle that for our purposes only depends on the magnitude of the vector $\mathbf{k}$, and μ_σ is the chemical potential. In the case of electrons the index σ specifies the spin of the electron, while for the case of quarks it specifies the spin, color and flavor of the quark. Hence, the quasiparticle energy and the effective interaction between quasiparticles are defined as

$$\epsilon_\sigma(\mathbf{k}) - \mu_\sigma \equiv \frac{\delta\Omega}{\delta N_\sigma(\mathbf{k})},$$
$$f_{\sigma\sigma'}(\mathbf{k},\mathbf{k}') \equiv \frac{\delta\Omega}{\delta N_\sigma(\mathbf{k})\delta N_{\sigma'}(\mathbf{k}')}.$$

An important quantity in Fermi-liquid theory is the effective mass m_σ^* of a quasiparticle of species σ near its Fermi surface. It is defined in terms of the group velocity v_σ^* evaluated at the Fermi momentum k_σ

$$m_\sigma^* \equiv \frac{k_\sigma}{v_\sigma^*} \equiv k_\sigma\left[\frac{\partial\epsilon_\sigma(\mathbf{k})}{\partial k}\right]_{k=k_\sigma}^{-1}, \quad (2)$$

such that upon linearizing the quasiparticle energy around the Fermi surface we obtain

$$\epsilon_\sigma(\mathbf{k}) \simeq \mu_\sigma + \frac{k_\sigma}{m_\sigma^*}(k - k_\sigma), \quad (3)$$

with $\mu_\sigma = \epsilon_\sigma(k_\sigma)$ as the Fermi energy of species σ. In the noninteracting limit, the effective mass reduces to
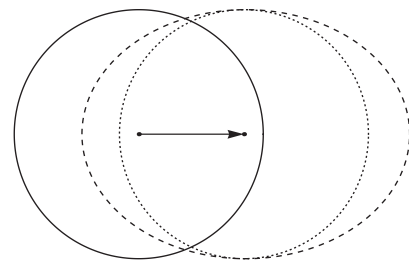

FIG. 1. A Galilean transformation (dotted curve) and Lorentz boost (dashed curve) of a Fermi sphere (solid curve). The boosts have been scaled in order to compare the shapes of the Fermi sphere after the transformation. The volume of the Fermi sphere, i.e., the density of the gas, becomes larger due to the Lorentz contraction.

$m_\sigma^* = m_\sigma$ and $m_\sigma^* = \epsilon_{\sigma 0}(k_\sigma) = \sqrt{k_\sigma^2 + m_\sigma^2}$ for nonrelativistic and relativistic dispersions, respectively.

Using the fact that the pressure is an invariant under Galilean or Lorentz transformations (see Appendix B 1), of which the effect can be written as a change in the distribution as shown in Fig. 1, Eq. (1) should give zero for this particular choice of $\delta N_\sigma(\mathbf{k})$ and hence relate $\epsilon_\sigma(\mathbf{k})$ to $f_{\sigma\sigma'}(\mathbf{k}, \mathbf{k}')$. In other words, by performing an infinitesimal Galilean or Lorentz transformation on the Fermi sphere, the effective mass can be related to the effective interaction at the Fermi surface [1,27].

To this end, consider an infinitesimal change in the Fermi surface from k_σ to $k_\sigma + \delta k_\sigma(\hat{\mathbf{k}})$

$$\delta N_\sigma(\mathbf{k}) = \begin{cases} 1 & k_\sigma \le k \le k_\sigma + \delta k_\sigma(\hat{\mathbf{k}}) & \delta k_\sigma > 0, \\ -1 & k_\sigma + \delta k_\sigma(\hat{\mathbf{k}}) \le k \le k_\sigma & \delta k_\sigma < 0, \\ 0 & \text{otherwise}, \end{cases}$$

where the change in the Fermi surface solely depends on the direction in momentum space denoted by $\hat{\mathbf{k}}$. The corresponding change in the thermodynamic potential density can be written as

$$\delta\Omega = \sum_\sigma \int \frac{d\hat{\mathbf{k}}}{(2\pi)^3} \int_{k_\sigma}^{k_\sigma + \delta k_\sigma} dk k^2 [\epsilon_\sigma(\mathbf{k}) - \mu_\sigma] + \frac{1}{2} \sum_{\sigma,\sigma'} \iint \frac{d\hat{\mathbf{k}}}{(2\pi)^3} \frac{d\hat{\mathbf{k}}'}{(2\pi)^3} \int_{k_\sigma}^{k_\sigma + \delta k_\sigma} dk k^2$$

$$\times \int_{k_{\sigma'}}^{k_{\sigma'} + \delta k_{\sigma'}} dk' k'^2 f_{\sigma\sigma'}(\mathbf{k}, \mathbf{k}') - \sum_\sigma n_\sigma \delta\mu_\sigma$$

$$= \sum_\sigma \frac{k_\sigma^3}{4\pi^2 m_\sigma^*} \int \frac{d\hat{\mathbf{k}}}{4\pi} \delta k_\sigma^2(\hat{\mathbf{k}}) + \sum_{\sigma,\sigma'} \frac{k_\sigma^2 k_{\sigma'}^2}{2(2\pi^2)^2} \iint \frac{d\hat{\mathbf{k}}}{4\pi} \frac{d\hat{\mathbf{k}}'}{4\pi} f_{\sigma\sigma'}(k_\sigma, k_{\sigma'}, \theta) \delta k_\sigma(\hat{\mathbf{k}}) \delta k_{\sigma'}(\hat{\mathbf{k}}') - \sum_\sigma n_\sigma \delta\mu_\sigma. \quad (4)$$

In the second line the integrals were expanded to second order in $\delta k_\sigma(\hat{\mathbf{k}})$, and $f_{\sigma\sigma'}(k_\sigma, k_{\sigma'}, \theta)$ was defined as the effective interaction at the Fermi surfaces between two species, with θ the angle between the directions of $\mathbf{k}$ and $\mathbf{k}'$. Next we expand δk_σ in terms of spherical harmonics and $f_{\sigma\sigma'}$ in terms of Legendre polynomials as

$$\delta k_\sigma(\hat{\mathbf{k}}) = \sum_{l,m} \delta k_\sigma^{lm} Y_{lm}(\hat{\mathbf{k}}),$$

$$f_{\sigma\sigma'}(k_\sigma, k_{\sigma'}, \theta) = \sum_l f_{l,\sigma\sigma'}(k_\sigma, k_{\sigma'}) P_l(\cos\theta).$$

For an imbalanced system, the difference in density n_σ results in a difference in μ_σ, which can cause m_σ^* to be different from each other even if their noninteracting bare masses m_σ are the same. For each species, the particle density obeys $n_\sigma = k_\sigma^3/6\pi^2$. Inserting these expansions and using the orthogonality of the spherical harmonics, Eq. (4) becomes

$$\delta\Omega = -\sum_\sigma n_\sigma \delta\mu_\sigma + \sum_{l,m,\sigma} \frac{3n_\sigma |\delta k_\sigma^{lm}|^2}{2m_\sigma^*}$$

$$+ \sum_{l,m,\sigma,\sigma'} \frac{f_{l,\sigma\sigma'}(k_\sigma, k_{\sigma'}) k_\sigma^2 k_{\sigma'}^2 \delta k_\sigma^{lm} (\delta k_{\sigma'}^{lm})^*}{8\pi^4 (2l+1)}. \quad (5)$$

In the balanced case, all Fermi momenta are the same, $k_\sigma = k_F$, $\delta k_\sigma^{lm} = \delta k_F^{lm}$, then Eq. (5) reduces to

$$\delta\Omega = -n\delta\mu + \sum_{l,m} \frac{3n}{2m^*} |\delta k_F^{lm}|^2 \left[1 + \frac{F_l}{2l+1}\right], \quad (6)$$

where the intensive quantities m^*, μ, k_F and F_l are the same for all species, and n is the total density, i.e., the density summed over all species. The (dimensionless) Landau Fermi-liquid parameters F_l are defined as

$$F_l = \sum_{\sigma'} \frac{k_F^2 f_{l,\sigma\sigma'}(k_F)}{2\pi^2} \left[\frac{\partial\epsilon(\mathbf{k})}{\partial k}\right]_{k_F}^{-1} = \sum_{\sigma'} \frac{k_F m^* f_{l,\sigma\sigma'}(k_F)}{2\pi^2}. \quad (7)$$

Note that F_l is species independent, but the interspecies and intraspecies interactions can be different, so the subscript σ is shown explicitly in $f_{l,\sigma\sigma'}$ but not in F_l. From the above it is possible to derive the equation for the effective mass, as we first show for the simpler balanced case.

Consider a change in the distribution due to a Lorentz transformation as shown in Fig. 1. The shape of the Fermi sphere is determined from the equation $\mu = -k_\mu u^\mu$, where $k^\mu = (\epsilon(\mathbf{k}), \mathbf{k})$ is the four-momentum, $u^\mu = (\gamma, \gamma\mathbf{v})$ is the four-velocity of the Fermi sphere with the Lorentz factor $\gamma = 1/\sqrt{1 - v^2}$. The minus sign in the previous expression and in $u_\mu u^\mu = -1$ are a consequence of our choice of the metric $\eta_{\mu\nu} = \text{diag}(-1, 1, 1, 1)$. In the rest frame, where $u^\mu = (1, \mathbf{0})$, the above reduces to the condition $\epsilon(k_F) = \mu$. Similarly, the shape of the Fermi surface can be determined from the Lorentz transformation of the momentum to a frame moving with velocity $-\mathbf{v}$,

$$\mathbf{k} \rightarrow \mathbf{k} - \hat{\mathbf{v}}(\hat{\mathbf{v}} \cdot \mathbf{k})(1 - \gamma) + \epsilon(\mathbf{k})\mathbf{v}\gamma,$$

which for an infinitesimal Lorentz transformation reduces to $\mathbf{k} \rightarrow \mathbf{k} + \epsilon(\mathbf{k})\mathbf{v}$ and in the nonrelativistic limit to $\mathbf{k} \rightarrow \mathbf{k} + m\mathbf{v}$. Note that the deformation of the Fermi sphere due to the Lorentz contraction shows up only in higher-order terms of $\mathbf{v}$.

First, consider the nonrelativistic case in which an infinitesimal Galilean transformation shifts all momenta from $\mathbf{k}$ to $\mathbf{k} + m\mathbf{v}$. This results in a change of the Fermi surface according to $\delta k_F = m\hat{\mathbf{k}} \cdot \mathbf{v} = mv Y_{10}(\cos\theta)/\sqrt{3}$,

such that $\delta k_F^{lm} = \delta_{l1}\delta_{m0}mv/\sqrt{3}$. Furthermore, the total energy of the system transforms as $E \rightarrow E + \frac{1}{2}Mv^2$, where M is the total mass of the system, which induces a change in the chemical potential $\mu = \partial E/\partial N \rightarrow \mu + \frac{1}{2}mv^2$. Inserting this into Eq. (6) gives the well-known Landau effective-mass relation in the balanced case [1–4]

$$m^* = m\left(1 + \frac{1}{3}F_1\right). \tag{8}$$

Secondly, for a relativistic system the momenta are shifted by $\mathbf{k} \rightarrow \mathbf{k} + \epsilon(\mathbf{k})\mathbf{v}$ such that $\delta k_F^{lm} = \delta_{l1}\delta_{m0}\mu v/\sqrt{3}$. Since the total energy of the system transforms as $E \rightarrow \gamma E \simeq E + \frac{1}{2}Ev^2$, the change in the chemical potential is $\delta\mu = \frac{1}{2}\mu v^2$. Inserting these into Eq. (6) gives the relativistic Landau effective-mass relation [27]

$$m^* = \mu\left(1 + \frac{1}{3}F_1\right). \tag{9}$$

Note that in the right-hand side F_1 also depends on μ, because the Fermi momentum k_F is a, in general complicated, function of μ.

Now for the more general imbalanced case. Since the Lorentz transformation is applied uniformly to each species, according to the symmetry of the formula, we can expect that the contribution from each species in Eq. (5) should vanish, namely,

$$\frac{n_\sigma \mu_\sigma^2 v^2}{2m_\sigma^*} + \sum_{\sigma'} \frac{f_{1,\sigma\sigma'}(k_\sigma, k_{\sigma'})k_\sigma^2 k_{\sigma'}^2 \mu_\sigma \mu_{\sigma'} v^2}{72\pi^4}$$
$$- \frac{n_\sigma \mu_\sigma v^2}{2} = 0.$$

Then we get the general expression for the effective mass,

$$m_\sigma^* = \mu_\sigma\left[1 + \sum_{\sigma'} \frac{f_{1,\sigma\sigma'}(k_\sigma, k_{\sigma'})N_{\sigma'}(0)}{3}\frac{\mu_{\sigma'}k_{\sigma'}m_\sigma^*}{\mu_\sigma k_\sigma m_{\sigma'}^*}\right], \tag{10}$$

where $N_\sigma(0) = m_\sigma^* k_\sigma/2\pi^2$ is the density of states at the Fermi energy of species σ. The arguments in f_1 emphasize that, in the imbalanced case, the interaction may depend not only on the angle between the momenta but also on the absolute value of the Fermi momentum of each species. In fact, the same expression of m_σ^* can be obtained more strictly by considering the addition of a single particle to the system and comparing the energy increase in two different frames.

We can introduce the average effective mass, which is of practical importance, as $m^* = \sum_\sigma m_\sigma^*/N$ with N the total number of species. Correspondingly, the average chemical potential is $\mu = \sum_\sigma \mu_\sigma/N$. In order to get a similar expression as in Eq. (9), we introduce the relative weight of each species as $x_\sigma = \mu_\sigma/N\mu$ such that $\sum_\sigma x_\sigma = 1$, and

then generalize the Landau effective-mass relation with average values as

$$m^* = \mu\left[1 + \frac{1}{3}\sum_{\sigma\sigma'}f_{1,\sigma\sigma'}(k_\sigma, k_{\sigma'})N_{\sigma'}(0)\frac{x_{\sigma'}k_{\sigma'}m_\sigma^*}{k_\sigma m_{\sigma'}^*}\right], \tag{11}$$

where the double-sum term, which can be defined again as F_1, plays the role of the Landau parameter in the balanced case as in Eq. (9), therefore we obtain now

$$F_1 = \sum_{\sigma\sigma'}f_{1,\sigma\sigma'}(k_\sigma, k_{\sigma'})N_{\sigma'}(0)\frac{x_{\sigma'}k_{\sigma'}m_\sigma^*}{k_\sigma m_{\sigma'}^*},$$

which, obviously, reduces to Eq. (7) as the system becomes balanced.

In the following sections the effective mass will be derived from a microscopic RPA calculation. In particular, in Sec. VI it will be determined from the specific heat. The specific heat (per volume) for low temperatures can be expressed in terms of the effective masses by

$$C_V = \frac{1}{V}\left(\frac{\partial E}{\partial T}\right)_{V,N} = \frac{1}{V}\left[\sum_{k,\sigma}\frac{\partial E}{\partial N_\sigma(\mathbf{k})}\frac{\partial N_\sigma(\mathbf{k})}{\partial T}\right]_{V,N}$$
$$\simeq \sum_\sigma \frac{k_\sigma m_\sigma^*}{6}T = \sum_\sigma \frac{\pi^2}{3}N_\sigma(0)T, \tag{12}$$

where it was used that $\partial(E/V)/\partial N_\sigma(\mathbf{k}) = \partial\Omega/\partial N_\sigma(\mathbf{k}) + \mu_\sigma \equiv \epsilon_\sigma(\mathbf{k})$ and for the temperature derivative the Sommerfeld expansion was used, c.f. Eq. (E8). This result is a trivial generalization of the single species or balanced case, since the effective mass already contains the effect of interactions, such that the contribution to the heat capacity of a single quasiparticle is additive.

III. RANDOM PHASE APPROXIMATION

Our starting point is the partition function

$$Z = \int \mathcal{D}\bar{\psi}\,\mathcal{D}\psi\,\mathcal{D}A_\mu\,\mathcal{D}\bar{\eta}\,\mathcal{D}\eta \exp\left(-\int d^4x \mathcal{L}_{\text{QCD}}^{\text{E}}\right),$$

containing the Euclidean QCD Lagrangian density fixed in a linear gauge $f_\mu A_\mu^a = 0$,

$$\mathcal{L}_{\text{QCD}}^{\text{E}} = \sum_f \bar{\psi}_f(\gamma_\mu D_\mu + m_f - \gamma_0 \mu_f)\psi_f + \frac{1}{4}G_{\mu\nu}^a G_{\mu\nu}^a$$
$$+ \bar{\eta}^a(\partial_\mu f_\mu \delta^{ab} + gf^{abc}A_\mu^c f_\mu)\eta^b + \frac{1}{2\xi}(f_\mu A_\mu^a)^2,$$

where ψ_f is the quark field of flavor f (the color c and spin s degrees of freedom are not shown explicitly) with mass m_f and chemical potential μ_f, A_μ^a are the gluon fields, η^a are the ghost fields, g is the QCD coupling constant, ξ is a gauge-fixing parameter, f^{abc} are the fine-structure constants of the color SU(3) group, the covariant derivative $D_\mu = \partial_\mu - igt^a A_\mu^a$ and the antisymmetric gluon field tensor $G_{\mu\nu}^a = \partial_\mu A_\nu^a - \partial_\nu A_\mu^a + gf^{abc}A_\mu^b A_\nu^c$. For large densities, the fermionic degrees of freedom become

increasingly important, such that the large-N_F limit could give insight into the behavior of quarks at high densities. Therefore, consider the large-N_F limit with a fixed rescaled coupling $\tilde{g}^2 = g^2 N_F$,

$$
\begin{aligned}
\mathcal{L}_{\text{QCD}}^{\text{E}} = &\sum_f \bar{\psi}_f (\slashed{\partial} + m_f - \gamma_0 \mu_f - \tilde{g} N_F^{-(1/2)} i \gamma_\mu t^a A_\mu^a) \psi_f \\
&+ \frac{1}{2} A_\mu^a \left(\partial_\mu \partial_\nu - \partial^2 \delta_{\mu\nu} - \frac{1}{\xi} f_\mu f_\nu \right) A_\nu^a \\
&+ \bar{\eta}^a (\partial_\mu f_\mu \delta^{ab} + \tilde{g} N_F^{-(1/2)} f^{abc} A_\mu^c f_\mu) \eta^b \\
&+ \frac{1}{2} \tilde{g} N_F^{-(1/2)} (\partial_\mu A_\nu^a - \partial_\nu A_\mu^a) f^{abc} A_\mu^b A_\nu^c \\
&+ \frac{1}{4} \tilde{g}^2 N_F^{-1} f^{abc} f^{ade} A_\mu^b A_\nu^c A_\mu^d A_\nu^e,
\end{aligned}
$$

Integrating out the fermions and the ghosts gives

$$
\begin{aligned}
\mathcal{L}_{\text{QCD}}^{\text{eff}} = &-\text{Tr}_{c,f,s} \ln[-G_{0f}^{-1}(1 + \tilde{g} N_F^{-(1/2)} G_{0f} i \gamma_\mu t^a A_\mu^a)] \\
&- \text{Tr}_c \ln(\partial_\mu f_\mu \delta^{ab} + \tilde{g} N_F^{-(1/2)} f^{abc} A_\mu^c f_\mu) \\
&+ \frac{1}{2} A_\mu^a D_{0,\mu\nu}^{-1} \delta^{ab} A_\nu^b + \frac{1}{2} \tilde{g} N_F^{-(1/2)} (\partial_\mu A_\nu^a \\
&- \partial_\nu A_\mu^a) f^{abc} A_\mu^b A_\nu^c \\
&+ \frac{1}{4} \tilde{g}^2 N_F^{-1} f^{abc} f^{ade} A_\mu^b A_\nu^c A_\mu^d A_\nu^e,
\end{aligned}
$$

where the subscripts $\{c, f, s\}$ explicitly indicate that the trace should also be taken over color, flavor and spin space. When we expand the first line in N_F, the first-order contribution will vanish due to conservation of color, i.e., $\text{Tr}_c[t^a] = 0$. Only the second-order expansion in N_F of the first line will give a contribution. Thus, expansion in powers of N_F gives

$$
\begin{aligned}
\mathcal{L}_{\text{QCD}}^{\text{eff}} = &-\text{Tr}_{c,f,s} \ln(-G_{0f}^{-1}) - \text{Tr}_c \ln(\partial_\mu f_\mu \delta^{ab}) \\
&+ \frac{1}{2} A_\mu^a \left(D_0^{-1} + \sum_f \Pi_f \right)_{\mu\nu}^{ab} A_\nu^b + \mathcal{O}(N_F^{-(1/2)}),
\end{aligned}
$$

where we defined the polarization tensor $\Pi_{f,\mu\nu}^{ab}$ from the contribution of the quark with flavor f as

$$
\Pi_{f,\mu\nu}^{ab} = -g^2 \text{Tr}_{c,s} (G_{0f} \gamma_\mu t^a G_{0f} \gamma_\nu t^b),
$$

which is shown diagrammatically in Fig. 2. The polarization tensor $\Pi_{f,\mu\nu}^{ab}$ is diagonal in color space, as can be seen
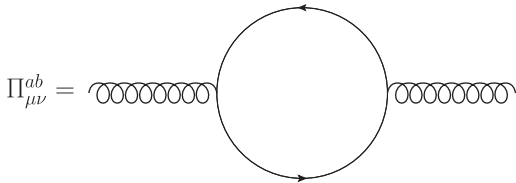

FIG. 2. The polarization tensor $\Pi_{\mu\nu}^{ab}$ to the first order.
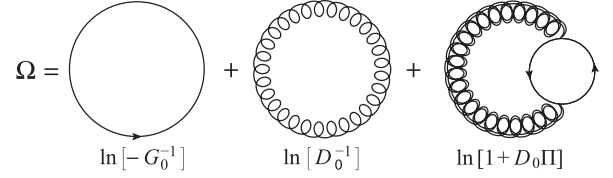

FIG. 3. The thermodynamic potential in the large-N_F or RPA approximation where the double gluon line signifies the dressed gluon propagator.

explicitly from Eq. (E1). Upon integrating out the gluons, the thermodynamic potential density is

$$
\begin{aligned}
\Omega(T, \{\mu_f\}) = &-V^{-1}\beta^{-1} \ln Z \\
\simeq &\frac{1}{V\beta} \Bigg\{ -N_C \text{Tr}_{f,s} \ln(-G_0^{-1}) \\
&+ \frac{N_G}{2} \text{Tr} \left[\ln(D_0^{-1}) - 2\ln(\partial_\mu f_\mu) - \ln\frac{1}{\xi} \right] \\
&+ \frac{N_G}{2} \text{Tr} \ln\left(1 + D_0 \sum_f \Pi_f \right) \Bigg\},
\end{aligned} \tag{13}
$$

where N_C is the number of colors, $N_G = N_C^2 - 1$ is the number of gluons, and we use the QCD values $N_C = 3$ and $N_G = 8$ in the following. The first two terms are the ideal Fermi and Bose gas contributions to the thermodynamic potential density, where the term $\text{Tr}\ln(\partial_\mu f_\mu)$ cancels the two unphysical degrees of freedom from $\text{Tr}\ln(D_0^{-1})$. The last term is the RPA correction (ring sum) to the thermodynamic potential density, as is shown in Fig. 3. Since we are mainly interested in the temperature dependence of Ω and the fact that the above definition contains (divergent) zero-temperature contributions, the $T = 0$ expression will be subtracted, i.e., we consider $\Delta\Omega(T, \{\mu_f\}) \equiv \Omega(T, \{\mu_f\}) - \Omega(0, \{\mu_f\})$. In Sec. IV, an example is considered to check the expression for the Landau effective mass analytically and in Sec. VI the above thermodynamic potential density is calculated numerically for the case of a two-flavor imbalanced quark system.

IV. FERMI-LIQUID PARAMETERS IN WEAK COUPLING

In the limit of weak coupling the interaction contribution to the thermodynamic potential density is given solely by the exchange diagram

$$
\Omega_{\text{int}} = \frac{N_G}{2V\beta} \sum_f \text{Tr}(D_0 \Pi_f).
$$

Using the definition of the free gluon propagator in the Lorentz gauge, this can be written as

$$\Omega_{\text{int}} = \frac{N_G}{2\beta} \sum_f \sum_{\omega_q} \int \frac{d^3q}{(2\pi)^3} \frac{\Pi_{f,\mu\mu}(i\omega_q, \mathbf{q})}{\omega_q^2 + q^2}$$

$$= g^2 \frac{N_G}{4} \sum_f \sum_{s_1,s_2,s_3=\pm 1} \int \frac{d^3p\, d^3q}{(2\pi)^6} \mathcal{F}^f_{s_1,s_2,s_3}(\mathbf{p}, \mathbf{q})$$

$$\times [N^{s_2}_f(\mathbf{q})N^{s_3}_B(\mathbf{p}-\mathbf{q})(1 - N^{s_1}_f(\mathbf{p})) - N^{s_1}_f(\mathbf{p})$$

$$\times (1 - N^{s_2}_f(\mathbf{q}))(1 + N^{s_3}_B(\mathbf{p}-\mathbf{q}))],$$

where the Fermi and Bose distributions are defined as

$$N^s_f(\mathbf{p}) = \frac{1}{e^{\beta[s\epsilon_{0f}(\mathbf{p}) - \mu_f]} + 1}, \qquad N^s_B(\mathbf{p}) = \frac{1}{e^{\beta[s\epsilon^g(\mathbf{p})]} - 1},$$

respectively, the explicit expression for $\Pi_{f,\mu\mu}$ is shown in Eq. (E3), the Matsubara sum over the bosonic frequencies ω_q was performed, $\epsilon_{0f}(\mathbf{p}) = \sqrt{p^2 + m_f^2}$ denotes the free quark dispersion while $\epsilon^g(\mathbf{p}) = p$ is the free gluon dispersion, and the function $\mathcal{F}$ was defined as

$$\mathcal{F}^f_{s_1,s_2,s_3}(\mathbf{p}, \mathbf{q}) = \frac{s_3}{\epsilon_{0f}(\mathbf{p})\epsilon_{0f}(\mathbf{q})\epsilon^g(\mathbf{p}-\mathbf{q})} \frac{-\epsilon_{0f}(\mathbf{p})\epsilon_{0f}(\mathbf{q}) + s_1 s_2(\mathbf{p}\cdot\mathbf{q} + 2m^2)}{s_1\epsilon_{0f}(\mathbf{p}) - s_2\epsilon_{0f}(\mathbf{q}) - s_3\epsilon^g(\mathbf{p}-\mathbf{q})}, \tag{14}$$

which will soon be shown to play the role of the interaction between two quarks ($s_1 = s_2 = 1$), two antiquarks ($s_1 = s_2 = -1$) or a quark and an antiquark ($s_1 = -s_2 = 1$ or $s_1 = -s_2 = -1$) mediated by the emission or absorption of a gluon (depending on the sign of s_3 relative to s_1 and s_2).

The quasiparticle energy and effective interaction can be obtained by varying the thermodynamic potential with respect to the Fermi distribution. In the flavor-imbalanced case, the distributions depend only on the flavor but not on the color and spin indices. To distinguish between the different contributions for each particle species it can be checked that the multiplication factor $N_G/4$ could be written as $\sum_{c,c',s,s'} t^a_{cc'} t^a_{c'c}/8$, where s and s' are just dummy indices denoting the spin degrees of freedom, which are helpful to arrive at the following expressions. Note that Ω_{int} is independent of the spin index, and in fact the spin degrees of freedom has already been summed over in the expression for $\mathcal{F}$. Explicitly, we find for these quantities

$$\epsilon_{c,f,s}(\mathbf{k}) - \mu_f \equiv \frac{\delta\Omega}{\delta N^+_{c,f,s}(\mathbf{k})}$$

$$= [\epsilon_{0f}(\mathbf{k}) - \mu_f] - \sum_{s'} \frac{g^2}{4} \sum_{c'} t^a_{cc'} t^a_{c'c} \sum_{s_2,s_3=\pm 1} \int \frac{d^3q}{(2\pi)^3} \mathcal{F}^f_{+,s_2,s_3}(\mathbf{k}, \mathbf{q})$$

$$\times [(1 + N^{s_3}_B(\mathbf{k}-\mathbf{q})(1 - N^{s_2}_f(\mathbf{q})) + N^{s_3}_B(\mathbf{k}-\mathbf{q}))N^{s_2}_f(\mathbf{q})], \tag{15}$$

$$f_{\{c,f,s\};\{c',f',s'\}}(\mathbf{k}, \mathbf{k}') \equiv \frac{\delta^2\Omega}{\delta N^+_{c,f,s}(\mathbf{k})\delta N^+_{c',f',s'}(\mathbf{k}')} = \frac{g^2}{4} t^a_{cc'} t^a_{c'c} \delta_{ff'} \sum_{s_3=\pm 1} \mathcal{F}^f_{+,+,s_3}(\mathbf{k}, \mathbf{k}'), \tag{16}$$

where $\sum_{c'} t^a_{cc'} t^a_{c'c} = \frac{N_G}{2N_C}$ and $t^a_{cc'} t^a_{c'c} = 1/2 - \delta_{cc'}/2N_C$, according to the definitions in Appendix A 1.

In the quasiparticle energy Eq. (15) the first term is the noninteracting part, while the second term corresponds to the quark self-energy, as is shown in Appendix G. The angular averaged interaction parameters are defined by the coefficients of the Legendre polynomial expansions of the effective interaction Eq. (16) evaluated on the Fermi sphere, by denoting $\cos\theta = \hat{\mathbf{k}} \cdot \hat{\mathbf{k}}'$,

$$f_{l;\{c,f,s\}} = \sum_{c',f',s'} f_{l;\{c,f,s\};\{c',f',s'\}} = \frac{2l+1}{2} \sum_{c',f',s'} \int d\theta \sin\theta f_{\{c,f,s\};\{c',f',s'\}}(\hat{\mathbf{k}}k_f, \hat{\mathbf{k}}'k_{f'})P_l(\cos\theta),$$

which gives for the zeroth and first interaction parameters

$$f_{0;f} = \frac{g^2 N_G N_S}{8N_C} \frac{1}{\mu_{0f}^2}\left[1 + \frac{\lambda^2 + 2m_f^2}{4k_f^2}\ln\left(\frac{\lambda^2}{\lambda^2 + 4k_f^2}\right)\right],$$

$$f_{1;f} = \frac{g^2 N_G N_S}{8N_C} \frac{3}{\mu_{0f}^2} \frac{\lambda^2 + 2m_f^2}{2k_f^2}\left[1 + \frac{\lambda^2 + 2k_f^2}{4k_f^2}\ln\left(\frac{\lambda^2}{\lambda^2 + 4k_f^2}\right)\right], \tag{17}$$

where $N_S = 2$ is the number of spin degrees of freedom, and a regulatory gluon mass λ was introduced, i.e., $\epsilon_k^g = \sqrt{k^2 + \lambda^2}$. We see that in this approximation the interaction is color- and spin-independent. For the sake of simplicity, therefore, we from now on omit the unnecessary color and spin indices, and use k_f and μ_{0f} for the Fermi momentum and the noninteracting Fermi energy of the quark with flavor f. The effective mass of the balanced case, Eq. (9), can be obtained from the interaction parameters Eq. (17) and (7) by expanding to the first order in the coupling constant

$$m^* = \mu + \sum_{\sigma'} \frac{\mu}{3} \frac{k_F m^*}{2\pi^2} f_{1,\sigma\sigma'} = \mu + \frac{k_F \mu_0^2}{6\pi^2} f_1 + \mathcal{O}(g^4),$$

(18)

where it was used that $\mu = \mu_0 + \mathcal{O}(g^2)$ as follows from Eq. (15). For the imbalanced case, a similar result can be obtained for each species according to Eq. (10),

$$m_f^* = \mu_f + \frac{\mu_f f_{1;f}(k_f) N_f(0)}{3} \approx \mu_f + \frac{k_f \mu_{0f}^2}{6\pi^2} f_{1;f}(k_f),$$

(19)

where the Kronecker delta $\delta_{ff'}$ in the interaction simplifies the expression considerably, such that we obtain the similar expression as in Eq. (18).

As a special case, we can use the above results to discuss a two-flavor imbalanced system, where the average effective mass and chemical potential can be defined as $m^* = (m_+^* + m_-^*)/2$ and $\mu = (\mu_+ + \mu_-)/2$ with the subscripts $+$ and $-$ for the majority and minority flavors, respectively. The imbalance can be quantified as $h = (\mu_+ - \mu_-)/(\mu_+ + \mu_-)$. For small imbalance, the factors $k_{\pm} f_{1;\pm}$ can be expanded in h with respect to the value in the balanced case, namely $k_{\pm} f_{1;\pm}(k_{\pm}) \approx k_F f_1(k_F) \times (1 \pm \Delta_{1\pm} h + \Delta_{2\pm} h^2)$. Note that the linear coefficients of the expansion can, in general, be different for each flavor. We obtain the expression of m^* for small h

$$m^* = \mu + \frac{k_F \mu^2 f_1(k_F)}{12\pi^2} [2 + (\Delta_{1+} - \Delta_{1-})h + (2 + 2\Delta_{1+} + 2\Delta_{1-} + \Delta_{2+} + \Delta_{2-})h^2 + \mathcal{O}(h^3)],$$

where the h^2 term is kept since the linear term may vanish for the symmetric case, namely $\Delta_{1+} = \Delta_{1-}$, and we have replaced μ_0 with μ because the difference is in higher-order of g. Compared with Eq. (11), the effective Landau parameter for the average effective mass is

$$F_1 = \frac{k_F \mu f_1(k_F)}{4\pi^2} [2 + (\Delta_{1+} - \Delta_{1-})h + (2 + 2\Delta_{1+} + 2\Delta_{1-} + \Delta_{2+} + \Delta_{2-})h^2 + \mathcal{O}(h^3)].$$

Similarly, we can obtain the effective mass difference $\Delta_{m^*} = (m_+^* - m_-^*)/2$ as a function of h:

$$\Delta_{m^*} = \mu h + \frac{k_F \mu^2 f_1(k_F)}{12\pi^2} [(4 + \Delta_{1+} + \Delta_{1-})h + (2\Delta_{1+} - 2\Delta_{1-} + \Delta_{2+} - \Delta_{2-})h^2 + \mathcal{O}(h^3)].$$

It is quite natural to find $\Delta_{m^*} \propto h$ in the leading order.

The consistency of the above results will now be verified to the lowest order in the coupling constant using the quark self-energy. Starting from the dispersion and self-energy of Eq. (15), the effective mass in Eq. (18) or Eq. (19) can also be derived in a different manner. The quasiparticle pole of the quark propagator is

$$\epsilon_f(\mathbf{p}) \equiv \epsilon_{0f}(\mathbf{p}) + \Sigma_{c,f,s}^+(\epsilon_{0f}(\mathbf{p}) - \mu, \mathbf{p}),$$

where Σ^+ is the renormalized positive-energy projected self-energy. The effective mass corresponding to this pole is most easily defined from the Fermi velocity of the quasiparticle

$$\frac{m_f^*}{\mu_f} \equiv \frac{k_f}{v_f^* \epsilon_f} = k_f \left[\frac{1}{\epsilon_f(\mathbf{p})} \left(\frac{\partial \epsilon_f(\mathbf{p})}{\partial p} \right)^{-1} \right]_{p=k_f}.$$

Inserting the definition of the quasiparticle pole into the above gives, using $\partial \epsilon_{0f}(\mathbf{p})/\partial p = p/\epsilon_{0f}(\mathbf{p})$,

$$m_f^* = \mu_f k_f \left[\epsilon_{0f}(\mathbf{p}) \frac{\partial \epsilon_{0f}(\mathbf{p})}{\partial p} \right.$$
$$\left. + \frac{\partial \epsilon_{0f}(\mathbf{p}) \Sigma_{c,f,s}^+(\epsilon_{0f}(\mathbf{p}) - \mu_f, \mathbf{p})}{\partial p} \right]_{p=k_f}^{-1} + \mathcal{O}(g^4)$$
$$= \mu_f - \left[\frac{\partial \epsilon_{0f}(\mathbf{p}) \Sigma_{c,f,s}^+(\epsilon_{0f}(\mathbf{p}) - \mu_f, \mathbf{p})}{\partial \epsilon_{0f}(\mathbf{p})} \right]_{p=k_f} + \mathcal{O}(g^4).$$

(20)

Using that the explicit form of the self-energy in the zero-temperature limit can be written as (c.f. Eq. (G2))

$$\Sigma_{c,f,s}^+(\epsilon_{0f}(\mathbf{p}) - \mu_f, \mathbf{p})$$
$$= \sum_{c',f',s'} \int \frac{d^3 q}{(2\pi)^3} f_{\{c,f,s\};\{c',f',s'\}}(\mathbf{p}, \mathbf{q}) N_{f'}^+(\mathbf{q}),$$

and the relation Eq. (B1) between the vector derivatives of the effective interaction, the derivative in Eq. (20) can be rewritten as

$$\left[\frac{\partial p}{\partial \epsilon_{0f}(\mathbf{p})}\frac{\partial \epsilon_{0f}(\mathbf{p})\Sigma^+_{c,f,s}(\epsilon_{0f}(\mathbf{p})-\mu_f,\mathbf{p})}{\partial p}\right]_{p=k_f} = \frac{\mu_{0f}}{k_f}\left[\sum_{c',f',s'}\int\frac{d^3q}{(2\pi)^3}\hat{\mathbf{p}}\cdot\frac{\partial \epsilon_{0f}(\mathbf{p})f_{\{c,f,s\};\{c',f',s'\}}(\mathbf{p},\mathbf{q})}{\partial \mathbf{p}}N^+_{f'}(\mathbf{q})\right]_{p=k_f}$$

$$= -\frac{\mu_{0f}}{k_f}\int\frac{dq}{2\pi^2}q^2\epsilon_{0f}(\mathbf{q})\delta(q-k_f)\frac{1}{3}\left[3\int\frac{d\hat{\mathbf{q}}}{4\pi}\hat{\mathbf{p}}\cdot\hat{\mathbf{q}}\sum_{c',f',s'}f_{\{c,f,s\};\{c',f',s'\}}(\mathbf{p},\mathbf{q})\right]_{p=k_f}$$

$$= -\frac{k_f\mu^2_{0f}}{2\pi^2}\frac{f_{1;\{c,f,s\}}(k_f)}{3},$$

where partial integration was used and $\delta_{ff'}\partial_{\mathbf{q}}N^+_{f'}(\mathbf{q}) = -\delta_{ff'}\hat{\mathbf{q}}\delta(q-k_f)$ at zero temperature. Therefore Eq. (20) is identical to Eq. (19), which shows that the phenomenological Landau argument is indeed consistent with the microscopic diagrammatic calculation.

V. DRESSED GLUON PROPAGATOR

Before we start the calculation of the temperature dependence of the large-N_F thermodynamic potential, it is useful to examine the dressed gluon propagator, which is a crucial ingredient of the RPA theory. The most physical gauge to study the propagator is the Coulomb gauge, since its form results from considering linear response [13,14]. This is also by far the most used gauge in condensed-matter theory. In this gauge, the gluon propagator is [13]

$$D_{\mu\nu}(Q) = \frac{P^T_{\mu\nu}}{Q^2+G(Q)} + \frac{Q^2}{q^2}\frac{\delta_{\mu0}\delta_{\nu0}}{Q^2+F(Q)} + \frac{\xi Q^2}{q^4}\frac{Q_\mu Q_\nu}{Q^2}$$

$$\equiv D^T(Q)P^T_{\mu\nu} - D^L(Q)\delta_{\mu0}\delta_{\nu0} + \frac{\xi Q^2}{q^4}\frac{Q_\mu Q_\nu}{Q^2},$$

where $P^T_{\mu\nu}$ is the three-dimensional transverse projector defined in Appendix A 2, F and G are related to the longitudinal and transverse projections of $\Pi_{\mu\nu}$ including the contributions of various species as well as the vacuum. More details can be found in Appendix E.

Consider the spectral functions of the transverse and longitudinal propagator, which are defined by

$$\rho^{T,L}(\omega,\mathbf{q}) \equiv \frac{1}{\pi}\Im[D^{T,L}(\omega+i0,\mathbf{q})].$$

In general the spectral function depends on the gauge, however, the positions of the poles are gauge independent, and the Coulomb gauge has the additional property $\rho^{T,L}(\omega,\mathbf{q}) > 0$ for $\omega > 0$ as required of a physical spectral function. For the balanced case, the spectral functions are shown in Fig. 4 for several values of μ and in Fig. 5 for several values of T. The latter includes a small-T correction to F and G, see Eq. (E9) [28]. The transverse and longitudinal plasmon modes and the large contribution due to the decay of the gluon into the particle-hole continuum $(0 < \omega < q)$ are clearly visible. Note that massless quarks are used in the limit of high density, c.f. Appendix E. However, a small but finite quark mass is necessary to renormalize the real part of the polarization tensor of the

vacuum, as shown in Eq. (E7). Since the vacuum contribution plays no significant role in the following calculation, we simply take this nonzero quark mass m in the vacuum term the same for different flavors.

For the two-flavor imbalanced case, it is clear from Eq. (13) that in the leading-order correction each flavor contributes separately to the polarization tensor. Because of the above setting, there is no mass imbalance in the present system, therefore it is enough to consider only positive h due to the symmetry. Following the notation in Sec. IV, all the above results can be easily generalized to such an imbalanced system by using $\mu(1 + h)$ to replace μ_+, and $\mu(1 - h)$ for μ_-. As $h \to 0$, the system reduces to
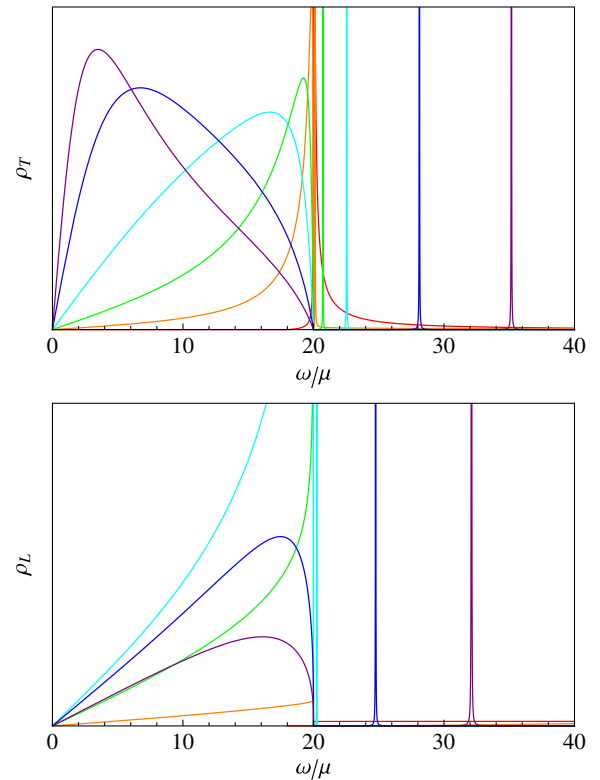

FIG. 4 (color online). The spectral function of the transverse (upper panel) and longitudinal (lower panel) gluon propagators as a function of frequency ω for several values of μ in the balanced case. Shown here for $T = 0$, $m = 1$, $q = 20$, $g = 1/2$, $N_F = 2$ and for different curves $\mu = 1, 20, 50, 100, 200, 300$ from red to purple.
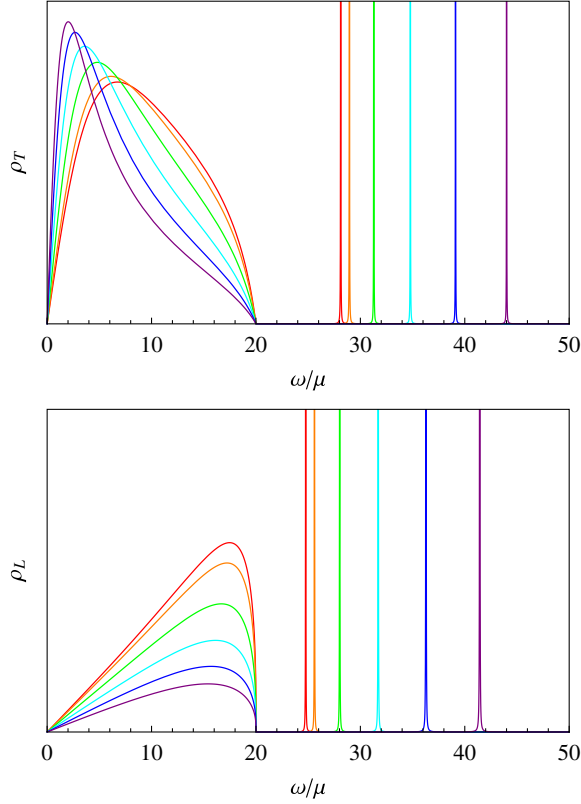
FIG. 5 (color online). The spectral functions of the transverse (upper panel) and longitudinal (lower panel) gluons as functions of ω for various T in the balanced case, with $\mu = 200$, $m = 1$, $q = 20$, $g = 1/2$, $N_F = 2$ and for different curves $T = 1, 40, 80, 120, 160, 200$ from red to purple. (In principle, T should be much smaller than μ, but here we show also large values of T to demonstrate the differences between the curves more clearly.)
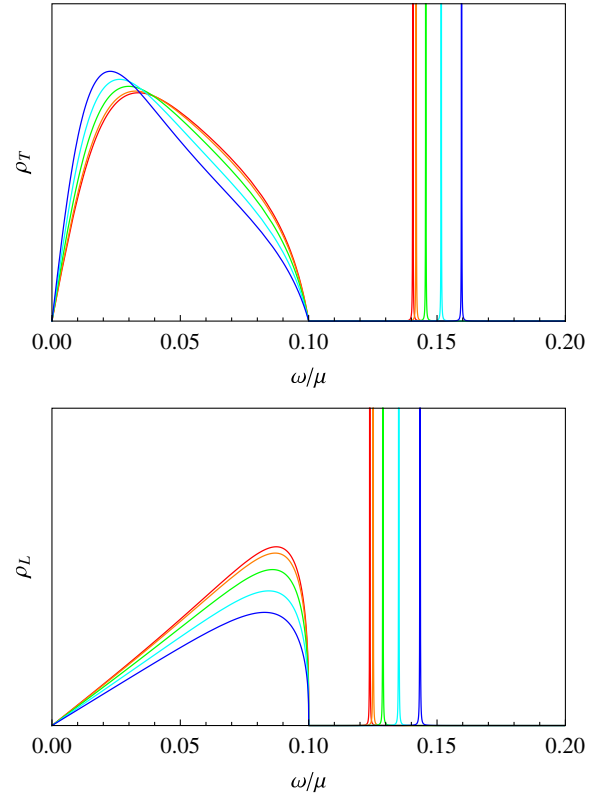
FIG. 6 (color online). The spectral functions of the transverse (upper panel) and longitudinal (lower panel) gluons as functions of ω for various h, with $T = 0$, $m = 0.001$, $q = 0.1$, $\mu = 1$, $g = 1/2$ and for different curves $h = 0, 0.2, 0.4, 0.6, 0.8$ from red to blue.

$$1 - \frac{2}{3} \frac{m_g^2}{\omega^2} \left(1 - \frac{\omega^2}{4\mu^2} \ln\frac{\omega^2}{4\mu^2} \right) = 0,$$

whose solution for small coupling constant yields $\omega_{\mathrm{pl}} \simeq \sqrt{2/3} m_g$ [13]. Here, m_g is the gluon thermal mass whose expression is obtained in the hard dense and hard thermal
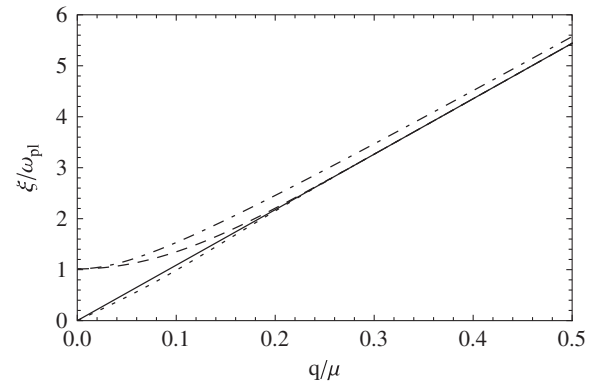

FIG. 7. The solutions of Eq. (21) at $T = h = 0$, with the dot-dashed curve for ξ^T, the dashed curve for ξ_2^L, and dotted curve for ξ_1^L. The solid line is a guide to the eye and corresponds to the dispersion of undressed gluons, $\omega = q$.

the balanced case. Now the low temperature condition requires $T \ll \mu(1 \pm h)$, such that h cannot be too close to 1, namely, the extremely imbalanced case. The spectral function for a two-flavor imbalanced system is shown for various h in Fig. 6. Comparing with Fig. 5, we see that increasing h has a similar effect as increasing T.

The dispersion relations of the modes can be found by solving

$$\Re[D_{T,L}^{-1}(\omega, q)] = 0. \tag{21}$$

In the transverse case there is a single solution $\xi^T(q) > q$, however, in the longitudinal case there are two solutions $\xi_1^L(q) < q < \xi_2^L(q)$, as shown in Fig. 7. Note that $\xi_1^L(q)$ is not a real propagating mode because the imaginary part in the region $0 < \omega < q$ is large due to particle-hole creation processes, as explained in Appendix E. The two plasmon modes $\xi^T(q)$ and $\xi_2^L(q)$ approach the so-called plasma frequency ω_{pl} as $q \to 0$. The plasma frequency of the transverse and longitudinal mode can be found by expanding the inverse propagators for small q and small ω, which in the zero-temperature limit gives for both cases

loop approximation as shown in Eq. (E10). In the limit $q \gg m_g \sim g\mu$ all solutions reduce to $\omega = q$, see Eq. (E11).

Furthermore, for the limit ω, $q \gg \mu$ the vacuum becomes increasingly dominant such that Eq. (21) has a zero at large Q called the Landau pole, $Q^2 = \exp(\frac{5}{3} + \frac{24\pi^2}{g^2 N_F})m^2 \equiv \Lambda_L^2$ [29], c.f. Eq. (E11), which, however, plays no role for our purpose as we are interested in the low-temperature behavior of the theory that is hardly influenced by the high-energy behavior of the gluon propagator. The dispersion relations for the case with nonzero T or h is similar but just with a little higher $m_{\rm pl}$. In fact, as a generalization of Eq. (E10), the thermal mass of a two-flavor imbalanced quark system reads

$$m_g^2 = \frac{g^2}{4\pi^2}\left[\mu^2(1+h)^2 + \mu^2(1-h)^2 + \frac{2\pi^2 T^2}{3}\right],$$

where h thus plays the same role as $\pi T/\sqrt{3}\mu$.

VI. THE FULL LARGE-N_F THERMODYNAMIC POTENTIAL

The full ideal-gas contribution to the thermodynamic potential density with the zero-temperature contribution subtracted is (c.f. Appendix F)

$$\Delta\Omega_0 = -N_C\left(N_F\frac{7\pi^2 T^4}{180} + \sum_f \frac{T^2\mu_f^2}{6}\right) - N_G\frac{T^4}{45\pi^2}.$$

The first part is the contribution of an ideal massless Fermi gas, while the second part is the Stefan-Boltzmann law of an ideal Bose gas. The RPA correction to Ω, the last term in Eq. (13), can be written as

$$\Omega_{\rm RPA}(T, \{\mu_f\}) = \frac{N_G}{2V\beta}\sum_{\omega_n, q}{\rm Tr}\ln(1 + D_0\Pi)$$
$$= \frac{N_G}{2V\beta}\sum_{\omega_n, q}\ln{\rm Det}\left(1 + \frac{FP^L}{Q^2} + \frac{GP^T}{Q^2}\right)$$
$$= \frac{N_G}{2V\beta}\sum_{\omega_n, q}\ln\left(1 + \frac{F}{Q^2}\right)\left(1 + \frac{G}{Q^2}\right)^2,$$

where the Lorentz gauge is used, while for the Coulomb gauge the second identity is not valid but the last result is still the same, which is a consequence of the gauge invariance of the thermodynamic potential density. Using contour deformations to carry out the Matsubara sum, as shown in Appendix D, we obtain

$$\Omega_{\rm RPA}(T, \{\mu_f\}) = \frac{N_G}{2\pi}\int\frac{dqd\omega}{(2\pi)^3}4\pi q^2[2N_B(\omega) + 1]$$
$$\times \{\Im[\ln\tilde{F}(\omega_+, \mathbf{q})] + 2\Im[\ln\tilde{G}(\omega_+, \mathbf{q})]\},$$

where $\tilde{F}(\omega_+, \mathbf{q}) = 1 + F(\omega_+, \mathbf{q})/(-\omega_+^2 + q^2)$, and similar for $\tilde{G}$ by replacing F with G. The temperature dependence can be obtained by subtracting the zero-temperature contribution. Since F and G contain corrections of order T^2, the leading-order correction in $\Delta\Omega_{\rm RPA}$ comes from two parts,

$$\Delta\Omega_{\rm RPA}(T, \{\mu_f\}) = \frac{N_G}{2\pi^3}\int dqd\omega q^2\left[N_B(\omega)\left(\arctan\frac{\Im(\tilde{F}^0)}{\Re(\tilde{F}^0)} + \pi\Theta[-\Re(\tilde{F}^0)]{\rm sgn}[\Im(\tilde{F})^0] + 2\arctan\frac{\Im(\tilde{G}^0)}{\Re(\tilde{G}^0)}\right.\right.$$
$$\left.\left. + 2\pi\Theta[-\Re(\tilde{G}^0)]{\rm sgn}[\Im(\tilde{G}^0)]\right)\frac{1}{2}[\Im(\ln\tilde{F}^T) - \Im(\ln\tilde{F}^0) + 2\Im(\ln\tilde{G}^T) - 2\Im(\ln\tilde{G}^0)]\right],$$

where the superscript T or 0 means the corresponding terms are taken at nonzero T or $T = 0$. We will refer to the first part as the N_B term and the second as the non-N_B term. The leading correction from the non-N_B term can be shown to be proportional to T^2 and is not of great interest in our study, since we will concentrate on the anomalous and dominant T dependence, which is a consequence of the N_B term. In the N_B term, the arctangent terms can be interpreted as contributions due to production and decay of thermal gluons, because of their dependence on the imaginary part of the gluon self-energies F and G, while the theta function terms are interpreted as a correction to the ideal gas law due to thermal plasmon modes.

The frequency integral over the theta function can be performed explicitly. In both the transverse and longitudinal case the sign of the imaginary part is positive when the

real part is negative, such that after the frequency integration the result of the integral is proportional to

$$T^4\int_0^\infty x^2\ln\frac{1 - e^{-\beta\xi_2(\beta^{-1}x)}}{1 - e^{-\beta\xi_1(\beta^{-1}x)}}dx,$$

where $x = q/T$ and $\xi_1 < \omega < \xi_2$ signifies the region where $\Re_{F,G} < 0$. In the limit of low temperature this integral will go to a constant. The theta-function contribution can thus be neglected since it is of higher order in the temperature than is of interest to us here.

Next we perform the integrals over the arctangents, whose structure at $T = h = 0$ is shown in Fig. 8. Note that, for the study of the leading-order T corrections, it is not necessary to include the T^2 term in F and G since the integral with $N_B(\omega)$ at low T is already in the order of T^2.
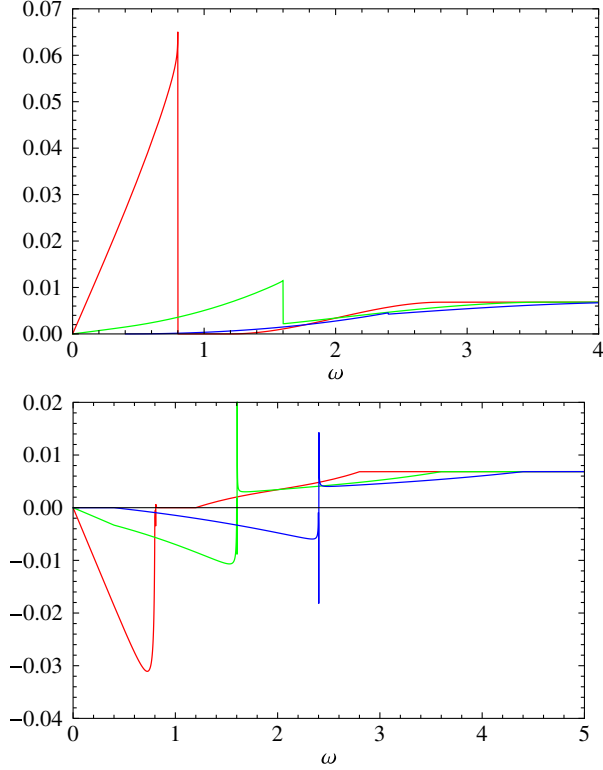
FIG. 8 (color online). The structure of $\arctan(\Im_F/\Re_F)$ (upper panel) and $\arctan(\Im_G/\Re_G)$ (lower panel) with $T = 0$, $m = 0.001\,\mu$, $h = 0$, $g = 1/2$, and for different curves, $q/\mu = 0.8$ (red), 1.6 (green), and 2.4 (blue), respectively. The contribution for $\max(0, q - 2\mu) < \omega < q$ is solely due to particle-hole contributions, while the contribution $q < \omega < \infty$ is due to particle-antiparticle processes (a combination of finite density and vacuum processes). The discontinuities at $\omega = q$ correspond to the plasmon modes shown in Fig. 7. The constant tails are due to the vacuum contribution, which, however, will not cause divergence because of the Bose distribution function $N_B(\omega)$.

The dominant contribution for small temperatures ($T \ll \mu$) comes from the frequency integration over the domain $\omega \in [0, q]$ for the case $q < 2\mu$, which is due to particle-hole creation. For the two-flavor balanced case ($N_F = 2$, $h = 0$), it was found numerically that the integral in the limit of small temperatures is

$$\frac{g^2\mu^2 T^2}{\pi^2}(c_1^L - c_2^L \ln g^2)$$

for the electric (longitudinal) gluons and

$$2\frac{g^2\mu^2 T^2}{\pi^2}\left(-c_1^T + c_2^T \ln\frac{g^2 T}{\mu}\right)$$

for the magnetic (transverse) gluons, with $c_1^L \simeq 0.48$, $c_2^L \simeq 0.16$, $c_1^T \simeq 0.42$, and $c_2^T \simeq 0.056$. These results are quite close to the analytic results for the leading-order correction terms at small g and T obtained in Ref. [30], where $c_1^L = [\ln(4\pi^2) - 1]/6 \approx 0.4460$, $c_2^L = 1/6 \approx 0.1667$,

$c_1^T = [\gamma_E - 6\zeta'(2)/\pi^2 + 3/2 + \ln(32\pi)]/18 \approx 0.4032$, and $c_2^T = 1/18 \approx 0.05556$.

For the imbalanced case, the above result for the transverse gluons can be generalized to

$$\frac{1}{2}\sum_{s=\pm1} 2\frac{g^2\mu^2(1 + sh)^2 T^2}{\pi^2}\left[-c_1^T + c_2^T \ln\frac{g^2 T}{\mu(1 + sh)}\right],$$

(22)

where the contributions from both flavors with chemical potentials $\mu(1 \pm h)$ are additive. The longitudinal part needs some further discussion. Since the static long-wavelength longitudinal modes are screened (c.f. Appendix E), the two chemical potentials contributing to $\Re_F$ can not be separated even in the lowest-order term. This is different from the result obtained in weak coupling, as shown in Eq. (16), where no interaction between the two flavors is involved. Therefore it is not surprising to find that a simple generalization of the balanced case, as $\sum_{s=\pm1} g^2\mu^2(1 + sh)^2 T^2(c_1^L - c_2^L \ln g^2)/2\pi^2$, does not fit well with the numerical results. To obtain a reasonable ansatz for the longitudinal part, we integrate the corresponding arctangent term of the imbalanced case in the low temperature limit up to $\mathcal{O}(g^2)$ to obtain

$$\frac{1}{2}\sum_{s=\pm1} \frac{g^2\mu^2(1 + sh)^2 T^2}{\pi^2}\left[\frac{1}{6}\ln\frac{4\pi^2(1 + sh)^2}{g^2(1 + h^2)} - \frac{1}{6}\right],$$

(23)

where we see that the factor $(1 + h^2) = \frac{1}{2}\sum_{s=\pm1}(1 + sh)^2$ is a mixture effect of the two flavors. This expression fits the numerical results very well with an error of only 3.5%. Furthermore, just based on the numerical data, we find another ansatz which fits the results even better

$$\frac{1}{2}\sum_{s=\pm1} \frac{g^2\mu^2(1 + sh)^2 T^2}{\pi^2}\left(c_1^L - c_2^L \ln\frac{g^2}{1 + sh}\right),$$

(24)

where the mixture effect is shown implicitly in the logarithm, since the denominator becomes dimensionless by canceling with the average chemical potential $\mu = \sum_{s=\pm1}\mu(1 + sh)/2$ in the numerator.

The specific heat (per volume) at fixed volume and particle number is [31]

$$C_V = T\left(\frac{\partial S}{\partial T}\right)_V = T\left(\frac{\partial S}{\partial T}\right)_{\mu_f} - \sum_f \frac{[(\partial n_f/\partial T)_{\mu_f}]^2}{(\partial n_f/\partial \mu_f)_T},$$

where the entropy density $S = (\partial\Omega/\partial T)_V$ and particle number density $n_f = -(\partial\Omega/\partial\mu_f)_V$. In the low-temperature limit the second term can be neglected, therefore the specific heat can be obtained, using Eqs. (22) and (23), as

$$C_V - C_V^0 = -T\left(\frac{\partial^2 \Delta\Omega}{\partial T^2}\right)_{\mu_f}$$

$$= -\frac{1}{2}\sum_{s=\pm 1}\frac{2g^2\mu^2(1+sh)^2 T}{\pi^2}$$

$$\times\left[\frac{1}{6}\ln\frac{4\pi^2(1+sh)^2}{g^2(1+h^2)}-\frac{1}{6}\right.$$

$$\left.- 2c_1^T + 3c_2^T + 2c_2^T\ln\frac{g^2 T}{\mu(1+sh)}\right], \quad (25)$$

where the specific heat $C_V^0 = -T(\partial^2\Delta\Omega_0/\partial T^2)_{\mu_f}$ of an ideal gas has been subtracted.

The effective mass and the first Landau parameter can be determined in the high-density limit by comparing Eq. (12) and (25),

$$m_\pm^* = \mu_\pm + \frac{g^2\mu(1\pm h)}{\pi^2}\left[\ln\frac{4\pi^2(1\pm h)^2}{g^2(1+h^2)}\right.$$

$$\left.- 1 - 12c_1^T + 18c_2^T + 12c_2^T\ln\frac{g^2 T}{\mu(1\pm h)}\right], \quad (26)$$

where we used $k_\pm = \mu_\pm = \mu(1\pm h)$ in the massless limit at high density. The first term in the effective mass is due to the ideal-gas specific heat. However, as pointed out before, the factor $(1+h^2)$ shows the mixing of the two flavors, unlike the weak-coupling results obtained in Sec. IV, e.g., Eq. (19). This is because, with the RPA correction, we incorporate the sum of an infinite chain of gluon self-energies, which incorporates interactions between different quark flavors. Since the longitudinal gluon is screened in the static long-wavelength limit, the mixing is even present in the low-T and small-g limit. The numerical fit in Eq. (24) also provides another expression for the effective mass,
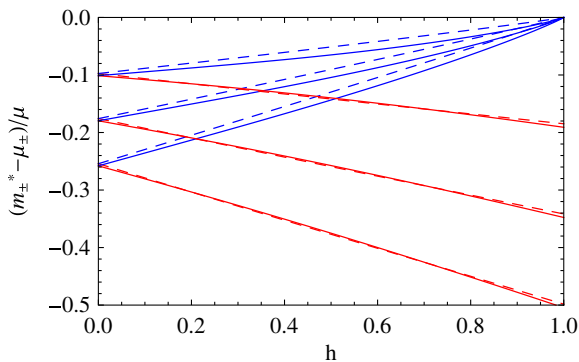

FIG. 9 (color online). The RPA correction to the effective mass as a function of h, with the red curves for the majority flavor (+) and the blue curves for the minority flavor (−). The solid curves correspond to the expression in Eq. (26) while the dashed curves to Eq. (27), and their difference is rather small. $g = 1/2$ and for each group of curves the temperature is $T/\mu = 10^{-6}$, 10^{-4} and 10^{-2} from bottom to top, respectively.

$$m_\pm^* = \mu_\pm + \frac{g^2\mu(1\pm h)}{\pi^2}\left[6c_1^L - 6c_2^L\ln\frac{g^2}{1\pm h}\right.$$

$$\left.- 12c_1^T + 18c_2^T + 12c_2^T\ln\frac{g^2 T}{\mu(1\pm h)}\right]. \quad (27)$$

As expected, all the above results return to the balanced case as $h \to 0$. As mentioned previously, the contribution from the non-N_B term is not included, which acts as a constant shift on the c_1^L and c_1^T factors. In Fig. 9, the change of effective mass due to the interaction is given as a function of imbalance at various temperatures. Finally, we emphasize again that h should not be too close to 1 even though the divergence from $\ln(1-h)$ is suppressed by the prefactor $(1-h)$, because in such an extremely imbalanced case the condition $T \ll \mu_-$ is not satisfied for the minority flavor.

VII. SUMMARY AND DISCUSSION

We have calculated the thermodynamic potential perturbatively in the large-N_F limit and the effective mass of the quarks is determined by using Fermi-liquid theory for an imbalanced cold dense quark system. The temperature dependence is obtained by using the gluon self-energy, from which the contributions from transverse and longitudinal gluons are explicitly shown. For the two-flavor imbalanced quark system, the effective mass is obtained both analytically within the weak-coupling limit, and numerically within the RPA approximation. We find that, in contrast to the weak-coupling result, where the effective mass of each flavor is independent of each other due to the lack of an interflavor interaction, the effective mass obtained from the RPA calculation depends on the chemical potentials of both flavors, which is a consequence of the static screening of the electric gluons at long wavelength.

From the RPA results, the logarithmic dependence on temperature of the specific heat and effective mass signals a breakdown of Fermi-liquid theory at zero-temperature. Non-Fermi-liquid behavior, due to unscreened long-range magnetic interactions, was already discussed several decades ago for the case of the electron gas [32,33]. In the large-N_F limit the QCD thermodynamic potential is essentially the same as that of QED, apart from group theory factors. The non-Abelian effects of QCD only show up if gluon self-interaction corrections are included. The logarithmic behavior in the balanced case has previously been seen in analytic and numerical calculations of the QCD thermodynamic potential and specific heat using the large-N_F limit, dimensional reduction, and hard-dense loop QCD perturbation theory [30,34–38]. We expect that such a logarithmic dependence shall have important effects on the imbalanced QCD phase diagram at low temperatures and directly influence the properties of quark matter in the core of neutron stars. As we pointed out in the introduction, with the effective masses and Landau

parameters obtained, we are now able to investigate how Landau Fermi-liquid theory modifies the properties of the various color superconducting phases. As a consequence of the color and flavor degrees of freedom, there can be many different kinds of pairing between quarks, of which some involve quarks with momenta of different magnitudes. Therefore, the results with imbalance we obtained here will play an important role to describe the competition between these imbalanced and superfluid phases. To better understand these effects, it is ultimately even necessary to go further, such as including the gluon self-interaction and extending our discussion to the three-flavor-imbalanced case. We hope progress along these directions will be achieved in the near future.

ACKNOWLEDGMENTS

APPENDIX A: CONVENTIONS

1. Euclidean conventions

The four-momentum vectors in Euclidean space-time will be written with capital letters $Q = (i(i\omega_n), \mathbf{q})$, while for the Wick-rotated case ($i\omega_n \rightarrow \omega + i0$) the roman capital letters $Q_+ = (i(\omega + i0), \mathbf{q})$ are used. Three momentum vectors are written in bold face $\mathbf{q}$ and its length as q. And $\omega \pm i0$ are sometimes written as $\omega_\pm$ for short.

The Euclidean gamma matrices in the standard representation are

$$\gamma_0 = \begin{pmatrix} 1 & 0 \\ 0 & -1 \end{pmatrix}, \qquad \gamma_i = -i\begin{pmatrix} 0 & \sigma_i \\ -\sigma_i & 0 \end{pmatrix},$$

$$\gamma_5 = \gamma_0\gamma_1\gamma_2\gamma_3 = \begin{pmatrix} 0 & 1 \\ 1 & 0 \end{pmatrix}.$$

All the above entries are 2×2 matrices and σ_i are the Pauli spin matrices

$$\sigma_1 = \begin{pmatrix} 0 & 1 \\ 1 & 0 \end{pmatrix}, \qquad \sigma_2 = \begin{pmatrix} 0 & -i \\ i & 0 \end{pmatrix},$$

$$\sigma_3 = \begin{pmatrix} 1 & 0 \\ 0 & -1 \end{pmatrix}.$$

The gamma matrices obey the following relations:

$$\{\gamma_\mu, \gamma_\nu\} = 2\delta_{\mu\nu}, \qquad \{\gamma_5, \gamma_\mu\} = 0, \qquad \gamma_5^2 = 1.$$

The charge conjugation matrix is

$$C = \gamma_0\gamma_2 = -i\begin{pmatrix} 0 & \sigma_2 \\ \sigma_2 & 0 \end{pmatrix},$$

which satisfies

$$C\gamma_\mu^T C = \gamma_\mu, \qquad C^T = C^{-1} = -C.$$

The eight generators of the fundamental representation of SU(3) are taken to be

$$t^1 = \frac{1}{2}\begin{pmatrix} 0 & 1 & 0 \\ 1 & 0 & 0 \\ 0 & 0 & 0 \end{pmatrix}, \qquad t^2 = \frac{1}{2}\begin{pmatrix} 0 & -i & 0 \\ i & 0 & 0 \\ 0 & 0 & 0 \end{pmatrix},$$

$$t^3 = \frac{1}{2}\begin{pmatrix} 1 & 0 & 0 \\ 0 & -1 & 0 \\ 0 & 0 & 0 \end{pmatrix}, \qquad t^4 = \frac{1}{2}\begin{pmatrix} 0 & 0 & 1 \\ 0 & 0 & 0 \\ 1 & 0 & 0 \end{pmatrix},$$

$$t^5 = \frac{1}{2}\begin{pmatrix} 0 & 0 & -i \\ 0 & 0 & 0 \\ i & 0 & 0 \end{pmatrix}, \qquad t^6 = \frac{1}{2}\begin{pmatrix} 0 & 0 & 0 \\ 0 & 0 & 1 \\ 0 & 1 & 0 \end{pmatrix},$$

$$t^7 = \frac{1}{2}\begin{pmatrix} 0 & 0 & 0 \\ 0 & 0 & -i \\ 0 & i & 0 \end{pmatrix}, \qquad t^8 = \frac{1}{2\sqrt{3}}\begin{pmatrix} 1 & 0 & 0 \\ 0 & 1 & 0 \\ 0 & 0 & -2 \end{pmatrix},$$

and have been normalized according to $\text{Tr}[t^a t^b] = \frac{1}{2}\delta^{ab}$. In general, the product of the generators is

$$t_{ij}^a t_{kl}^a = \frac{N_C - 1}{4N_C}(\delta_{ij}\delta_{kl} + \delta_{il}\delta_{kj})$$
$$- \frac{N_C + 1}{4N_C}(\delta_{ij}\delta_{kl} - \delta_{il}\delta_{kj}).$$

Furthermore, one will frequently encounter the following group-theory factors:

$$f^{abc}f^{abd} = N_C\delta^{cd}, \qquad \delta^{aa} = N_C^2 - 1 \equiv N_G,$$

$$t_{il}^a t_{lj}^a = \frac{N_C^2 - 1}{2N_C}\delta_{ij} = \frac{N_G}{2N_C}\delta_{ij},$$

in the above expressions N_C is the number of colors and N_G the number of gluons.

Fourier transforms are normalized as

$$\psi(\tau, \mathbf{x}) = \frac{1}{\sqrt{\beta}}\sum_n \int \frac{d^3p}{(2\pi)^{3/2}} \psi(i\omega_n, \mathbf{p})e^{i\mathbf{p}\cdot\mathbf{x} - i\omega_n\tau}$$

$$= \int \frac{d^4P}{\sqrt{\mathcal{V}}} \psi(P)e^{iP_\mu x_\mu},$$

where $\omega_n = \pi(2n + 1)/\beta$ are the fermionic Matsubara frequencies, $\mathcal{V} = \beta(2\pi)^3$ is the imaginary time phase space volume and $P_\mu = (i(i\omega_n), \mathbf{p})$ and $x_\mu = (\tau, \mathbf{x})$.

The Dirac equation in Euclidean space is

$$(\not\partial + m)\psi(x) = 0,$$

where $\not\partial = \gamma_\mu\partial_\mu$. In momentum space, the Dirac equation reads

$$(i\not P + m)\psi(P) = 0.$$

The eigenvalues of the matrix $i\not P$ are $\pm m$, since $(i\not P)^2 = -P^2 = m^2$. The eigenspinors corresponding to these eigenvalues are

$$i\not P u_s(\mathbf{p}) = -mu_s(\mathbf{p}), \qquad i\not P v_s(\mathbf{p}) = mv_s(\mathbf{p}).$$

Note that $i\not{p}$ is not a Hermitian matrix and that $v_s(-\mathbf{p})$ satisfies the same equation as $u_s(\mathbf{p})$. However, they can also be viewed as the eigenspinors of a Hermitian matrix

$$\gamma_0(i\mathbf{p}\cdot\vec{\gamma}+m)u_s(\mathbf{p}) = \epsilon_p u_s(\mathbf{p}),$$

$$\gamma_0(i\mathbf{p}\cdot\vec{\gamma}+m)v_s(-\mathbf{p}) = -\epsilon_p v_s(-\mathbf{p}).$$

The positive and negative energy eigenspinors have the following form:

$$u_s(\mathbf{p}) = \sqrt{\frac{\epsilon_p + m}{2\epsilon_p}}\begin{pmatrix} \xi_s \\ \frac{\mathbf{p}\cdot\vec{\sigma}}{\epsilon_p+m}\xi_s \end{pmatrix}, \tag{A1}$$

$$v_s(-\mathbf{p}) = \sqrt{\frac{\epsilon_p + m}{2\epsilon_p}}\begin{pmatrix} -\frac{\mathbf{p}\cdot\vec{\sigma}}{\epsilon_p+m}\xi_s \\ \xi_s \end{pmatrix}, \tag{A2}$$

where $\xi_\uparrow = (1,0)^T$ and $\xi_\downarrow = (0,1)^T$. They are orthonormal in the sense that

$$u_s^\dagger(\mathbf{p})u_{s'}'(\mathbf{p}) = v_s^\dagger(-\mathbf{p})v_{s'}'(-\mathbf{p}) = \delta_{ss'},$$

$$v_s^\dagger(-\mathbf{p})u_{s'}'(\mathbf{p}) = u_s^\dagger(-\mathbf{p})v_{s'}'(\mathbf{p}) = 0,$$

and satisfy the completeness relation

$$\sum_s[u_s(\mathbf{p})u_s^\dagger(\mathbf{p}) + v_s(-\mathbf{p})v_s^\dagger(-\mathbf{p})] = 1.$$

Using the above eigenspinors, the positive and negative energy projectors can be defined as

$$P_E^+(\mathbf{p}) \equiv \sum_s u_s(\mathbf{p})u_s^\dagger(\mathbf{p}) = \frac{\epsilon_p\gamma_0 - i\vec{\gamma}\cdot\mathbf{p} + m}{2\epsilon_p}\gamma_0,$$

$$P_E^-(\mathbf{p}) \equiv \sum_s v_s(-\mathbf{p})v_s^\dagger(-\mathbf{p}) = \frac{\epsilon_p\gamma_0 + i\vec{\gamma}\cdot\mathbf{p} - m}{2\epsilon_p}\gamma_0,$$

which in the massless case reduce to

$$P_E^s(\mathbf{p}, m=0) = \frac{1 + si\gamma_0\vec{\gamma}\cdot\hat{\mathbf{p}}}{2}.$$

The helicity projection operators project the spin along the momentum of the particle and read

$$\mathcal{P}^s(\mathbf{p}) = \frac{1 + s\mathbf{\Sigma}\cdot\hat{\mathbf{p}}}{2} = \frac{1 + si\gamma_5\gamma_0\vec{\gamma}\cdot\hat{\mathbf{p}}}{2},$$

where

$$\mathbf{\Sigma} = i\gamma_5\gamma_0\vec{\gamma} = \begin{pmatrix} \vec{\sigma} & 0 \\ 0 & \vec{\sigma} \end{pmatrix}$$

is the spin operator. Note that $[P_E^s(\mathbf{p})\gamma_0, \mathcal{P}^{s'}(\mathbf{p})] = 0$.

2. The Green's functions

The Green's functions of quarks and gluons in Euclidean space are defined by

$$G(\tau, \mathbf{x}; \tau', \mathbf{x}') = -\langle\psi(\tau, \mathbf{x})\bar{\psi}(\tau', \mathbf{x}')\rangle,$$

$$D_{\mu\nu}(\tau, \mathbf{x}; \tau', \mathbf{x}') = \langle A_\mu(\tau, \mathbf{x})A_\nu(\tau', \mathbf{x}')\rangle.$$

In momentum space, the free quark propagator is

$$G_0(P) = \frac{(i\omega_n + \mu)\gamma_0 - i\vec{\gamma}\cdot\mathbf{p} + m}{(i\omega_n + \mu)^2 - p^2 - m^2} = \frac{i\not{p} - m}{P^2 + m^2}.$$

In the Lorentz gauge ($\partial_\mu A_\mu = 0$), the momentum-space free gluon propagator is

$$D_{0,\mu\nu}(Q) = \frac{1}{Q^2}\left[\delta_{\mu\nu} - (1-\xi)\frac{Q_\mu Q_\nu}{Q^2}\right]$$

$$= \frac{P_{\mu\nu}}{Q^2} + \frac{\xi}{Q^2}\frac{Q_\mu Q_\nu}{Q^2},$$

while in the Coulomb gauge ($\partial_i A_i = 0$) it is [13]

$$D_{0,\mu\nu} = \frac{P_{\mu\nu}^T}{Q^2} + \frac{Q^2}{q^2}\frac{\delta_{\mu0}\delta_{\nu0}}{Q^2} + \xi\frac{Q^2}{q^4}\frac{Q_\mu Q_\nu}{Q^2},$$

where ξ is a gauge-fixing parameter and the projectors can be written as

$$P_{\mu\nu} = \delta_{\mu\nu} - \frac{Q_\mu Q_\nu}{Q^2}, \qquad P_{ij}^T = \delta_{ij} - \frac{\mathbf{q}_i\mathbf{q}_j}{q^2},$$

$$P_{\mu0}^T = P_{0\nu}^T = 0, \qquad P_{\mu\nu}^L = P_{\mu\nu} - P_{\mu\nu}^T.$$

Note that the free gluon propagator in the Lorentz gauge satisfies $Q_\mu D_{0,\mu\nu} = \xi Q_\nu/Q^2$, such that in the Landau gauge ($\xi = 0$) it is purely four-momentum transverse, i.e., $Q_\mu D_{0,\mu\nu} = 0$. The free gluon propagator in the Coulomb gauge satisfies $\mathbf{q}_i D_{0,i\nu} = \xi q^2 Q_\nu/Q^4$, such that in the Landau gauge it is three-momentum transverse. These propagators are diagonal in color space.

APPENDIX B: LORENTZ TRANSFORMATION PROPERTIES

In this section, the Lorentz transformation properties of some quantities are summarized, such as the thermodynamic potential, the distribution function and the effective interaction. The Lorentz transformation to a frame moving with velocity $\mathbf{v}$ is

$$\Lambda^{\mu\nu}(\mathbf{v}) = \begin{pmatrix} -\gamma & \cdots & -\gamma\mathbf{v}^T & \cdots \\ \vdots & \ddots & & \\ \gamma\mathbf{v} & & \delta_{ij} + \frac{\mathbf{v}_i\mathbf{v}_j}{v^2}(\gamma-1) & \\ \vdots & & & \ddots \end{pmatrix},$$

such that the four-momentum $P^\mu = (\epsilon(\mathbf{p}), \mathbf{p})$ of a particle transforms as

$$\begin{pmatrix} \epsilon(\mathbf{p}) \\ \mathbf{p} \end{pmatrix} \rightarrow \begin{pmatrix} \gamma(\epsilon(\mathbf{p}) - \mathbf{v}\cdot\mathbf{p}) \\ \mathbf{p} + \hat{\mathbf{v}}(\mathbf{p}\cdot\hat{\mathbf{v}})(\gamma-1) - \gamma\epsilon(\mathbf{p})\mathbf{v} \end{pmatrix}.$$

Not to be confused with the Dirac matrices γ^μ, the γ used in this section is the Lorentz factor $\gamma = 1/\sqrt{1-v^2}$.

1. Lorentz invariance of the thermodynamic potential density

The invariance of the thermodynamic potential density under Lorentz transformations can be shown using the stress-energy tensor. Consider the change in the thermodynamic potential density under a Lorentz transformation from the rest frame to a frame moving with velocity $\mathbf{v}$. Since an interacting gas of quarks in the rest frame is specified only by an energy density ρ and a pressure p, the stress-energy tensor is diagonal and of the form

$$T_{\mu\nu} = \mathrm{diag}(\rho, p, p, p)_{\mu\nu},$$

such that under a Lorentz transformation the thermodynamic potential density $\Omega = \rho - \mu n = -p$ changes as

$$\delta\Omega = \delta T_{00} - \delta(\mu n) = \gamma^2 v^2(\rho + p) - \delta(\mu n)$$
$$= \mu n\gamma^2 v^2 - \delta(\mu n).$$

The transformation of the chemical potential ($\mu = \partial E/\partial N$) follows from the Lorentz boosted total energy of the system $E \to \gamma(E - \mathbf{v} \cdot \mathbf{P}) = \gamma E$, where $\mathbf{P} = \mathbf{0}$ is the total momentum of the system in the rest frame, which results in $\mu \to \gamma\mu$. The transformation of the density is due to a Lorentz contraction in the volume $n \to \gamma n$. Thus the total change in μn is $\delta(\mu n) = (\gamma^2 - 1)\mu n = \gamma^2 v^2 \mu n$, such that under a Lorentz transformation $\delta\Omega = 0$. For an alternative derivation which uses the pressure transforms the same way as a force per area, see Ref. [39].

2. Transformation properties of $f(\mathbf{p}, \mathbf{p}')$

Consider the lowest-order correction to the free thermodynamic potential density

$$\Omega_{\mathrm{int}} = \frac{1}{2}\sum_{\sigma,\sigma'}\int\frac{d^3p\,d^3p'}{(2\pi)^3}f_{\sigma\sigma'}(\mathbf{p},\mathbf{p}')N_\sigma(\mathbf{p})N_{\sigma'}(\mathbf{p}').$$

Note that the distribution function $N(\mathbf{p})$ is a Lorentz invariant, which can be easily derived from the fact that the number of particles in a volume $d^3x\,d^3p$ of phase space is invariant under Lorentz transformations [40], i.e., $\tilde{N}(\tilde{\mathbf{p}}) = N(\mathbf{p})$ where the tilde signifies the Lorentz transformed quantity. Subsequently, it is possible to derive a transformation law for $f(\mathbf{p}, \mathbf{p}')$ by using that the distribution, the thermodynamic potential density and $d\mathbf{p}/\epsilon_0(\mathbf{p})$ are Lorentz invariant. It follows that $\epsilon_{0\sigma}(\mathbf{p})\epsilon_{0\sigma'}(\mathbf{p}')f_{\sigma\sigma'}(\mathbf{p},\mathbf{p}')$ should be Lorentz invariant, giving

$$\epsilon_{0\sigma}(\mathbf{p})\epsilon_{0\sigma'}(\mathbf{p}')f_{\sigma\sigma'}(\mathbf{p},\mathbf{p}') = \tilde{\epsilon}_{0\sigma}(\tilde{\mathbf{p}})\tilde{\epsilon}_{0\sigma'}(\tilde{\mathbf{p}}')\tilde{f}_{\sigma\sigma'}(\tilde{\mathbf{p}},\tilde{\mathbf{p}}'),$$

where $\epsilon_{0\sigma}(\mathbf{p}) = \sqrt{p^2 + m_\sigma^2}$. Expand $\tilde{f}$ to the lowest order in $\mathbf{v}$, using $\tilde{\epsilon}_0(\tilde{\mathbf{p}}) = \epsilon_0(\mathbf{p}) - \mathbf{v} \cdot \mathbf{p} + \mathcal{O}(v^2)$, $\tilde{\mathbf{p}} = \mathbf{p} - \epsilon_0(\mathbf{p})\mathbf{v} + \mathcal{O}(v^2)$, and $\mathbf{p}/\epsilon_0(\mathbf{p}) = \partial\epsilon_0(\mathbf{p})/\partial\mathbf{p}$,

$$f_{\sigma\sigma'}(\mathbf{p},\mathbf{p}') = \tilde{f}_{\sigma\sigma'}(\tilde{\mathbf{p}},\tilde{\mathbf{p}}')\left[1 - \mathbf{v}\cdot\frac{\mathbf{p}}{\epsilon_{0\sigma}(\mathbf{p})}\right]\left[1 - \mathbf{v}\cdot\frac{\mathbf{p}'}{\epsilon_{0\sigma'}(\mathbf{p}')}\right] + \mathcal{O}(v^2)$$

$$= \tilde{f}_{\sigma\sigma'}(\mathbf{p},\mathbf{p}') - \epsilon_{0\sigma}(\mathbf{p})\mathbf{v}\cdot\frac{\partial f_{\sigma\sigma'}(\mathbf{p},\mathbf{p}')}{\partial\mathbf{p}} - \epsilon_{0\sigma'}(\mathbf{p}')\mathbf{v}\cdot\frac{\partial f_{\sigma\sigma'}(\mathbf{p},\mathbf{p}')}{\partial\mathbf{p}'}$$

$$- f_{\sigma\sigma'}(\mathbf{p},\mathbf{p}')\left[\mathbf{v}\cdot\frac{\partial\epsilon_{0\sigma}(\mathbf{p})}{\partial\mathbf{p}} - \mathbf{v}\cdot\frac{\partial\epsilon_{0\sigma'}(\mathbf{p}')}{\partial\mathbf{p}'}\right] + \mathcal{O}(v^2)$$

$$= \tilde{f}_{\sigma\sigma'}(\mathbf{p},\mathbf{p}') - \mathbf{v}\cdot\left[\frac{\partial\epsilon_{0\sigma}(\mathbf{p})f_{\sigma\sigma'}(\mathbf{p},\mathbf{p}')}{\partial\mathbf{p}} + \frac{\partial\epsilon_{0\sigma'}(\mathbf{p}')f_{\sigma\sigma'}(\mathbf{p},\mathbf{p}')}{\partial\mathbf{p}'}\right] + \mathcal{O}(v^2).$$

If it is assumed that to the lowest order the interaction does not depend on any distribution functions, i.e., $\tilde{f}_{\sigma\sigma'}(\mathbf{p}, \mathbf{p}') = f_{\sigma\sigma'}(\mathbf{p}, \mathbf{p}')$, the above implies

$$\frac{\partial\epsilon_{0\sigma}(\mathbf{p})f_{\sigma\sigma'}(\mathbf{p},\mathbf{p}')}{\partial\mathbf{p}} = -\frac{\partial\epsilon_{0\sigma'}(\mathbf{p}')f_{\sigma\sigma'}(\mathbf{p},\mathbf{p}')}{\partial\mathbf{p}'}. \tag{B1}$$

Note that the above derivation is similar to that given in Ref. [27].

APPENDIX C: FROM MINKOWSKI TO EUCLIDIAN SPACE

In this section, we summarize how to turn the Minkowski quantum field theory of quantum chromodynamics into a Euclidean statistical field theory suitable for studying the dynamical properties of a many-particle system. The starting point is the gauge-fixed path integral for QCD

$$\int\mathcal{D}A_\mu\mathcal{D}\tilde{\psi}\mathcal{D}\psi\mathcal{D}\bar{\eta}\mathcal{D}\eta\exp\left\{i\int\mathcal{L}_{\mathrm{QCD}}d^4x\right\}, \tag{C1}$$

where A_μ are the gluon fields, ψ and $\bar{\psi} = i\psi^\dagger\gamma^0$ the quark fields, η and $\bar{\eta} = i\eta^\dagger\gamma^0$ the ghost fields and the QCD Lagrangian in Minkowski space fixed in a linear gauge ($f^\mu A_\mu^a = 0$) is given by

$$\mathcal{L}_{\text{QCD}} = -\sum_f [\bar{\psi}_f(\not{\partial} + m_f)\psi_f + ig\bar{\psi}_f\gamma^\mu t^a \psi_f A_\mu^a] - \frac{1}{2}A_a^\mu(\partial_\mu\partial_\nu - \partial^2\eta_{\mu\nu})A_a^\nu - \bar{\eta}^a\partial_\mu\partial^\mu\eta^a - gf^{abc}(\bar{\eta}^a\partial^\mu\eta^b)A_\mu^c$$

$$- \frac{1}{2}g(\partial^\mu A_a^\nu - \partial^\nu A_a^\mu)f^{abc}\eta_{\mu\sigma}\eta_{\nu\rho}A_b^\sigma A_c^\rho - \frac{1}{4}g^2 f^{abc}f^{ade}\eta_{\mu\sigma}\eta_{\nu\rho}A_a^\mu A_c^\nu A_d^\sigma A_e^\rho + \frac{1}{2\xi}(f^\mu A_\mu^a)^2, \tag{C2}$$

where ψ_f is the quark field with flavor f, and the summation over color and spin indices are shown implicitly. The metric was chosen to be $\eta_{\mu\nu} = \text{diag}(-1, 1, 1, 1)$ and the Minkowski gamma matrices in the standard representation are

$$\gamma^0 = -i\begin{pmatrix} 1 & 0 \\ 0 & -1 \end{pmatrix}, \qquad \gamma^i = -i\begin{pmatrix} 0 & \sigma_i \\ -\sigma_i & 0 \end{pmatrix}, \qquad \gamma^5 = i\gamma^0\gamma^1\gamma^2\gamma^3 = \begin{pmatrix} 0 & 1 \\ 1 & 0 \end{pmatrix}. \tag{C3}$$

The gamma matrices satisfy

$$\{\gamma^\mu, \gamma^\nu\} = 2\eta^{\mu\nu}, \qquad \{\gamma^5, \gamma^\mu\} = 0, \qquad (\gamma^5)^2 = 1.$$

By performing a Wick rotation, the above quantum field theory can be transformed into a statistical field theory. A Wick rotation amounts to taking an analytic continuation from real time to imaginary time ($t = -i\tau$), which turns the Minkowski metric $ds^2 = -dt^2 + dx^2$ into the Euclidean metric $ds^2 = d\tau^2 + dx^2$. To do this consistently, the zeroth component of all four-vectors need to change accordingly. The procedure is most easily understood by considering the length of the position four-vector

$$x^\mu x_\mu = x^\mu \eta_{\mu\nu} x^\nu = (t, \mathbf{x})\begin{pmatrix} -1 & 0 \\ 0 & \mathbb{1} \end{pmatrix}\begin{pmatrix} t \\ \mathbf{x} \end{pmatrix}$$

$$= (it, \mathbf{x})\mathbb{1}\begin{pmatrix} it \\ \mathbf{x} \end{pmatrix} \equiv x_\mu^E \delta_{\mu\nu} x_\nu^E,$$

$$x_\mu \eta^{\mu\nu} x_\nu = (-t, \mathbf{x})\begin{pmatrix} -1 & 0 \\ 0 & \mathbb{1} \end{pmatrix}\begin{pmatrix} -t \\ \mathbf{x} \end{pmatrix}$$

$$= (it, \mathbf{x})\mathbb{1}\begin{pmatrix} it \\ \mathbf{x} \end{pmatrix} \equiv x_\mu^E \delta_{\mu\nu} x_\nu^E,$$

where it is seen that the minus sign of the Minkowski metric is absorbed in the definition of the Euclidean four-vectors $x_\mu^E = (it, \mathbf{x}) = (\tau, \mathbf{x})$. In Euclidean space, no distinction is made between upper and lower indices. A simple way to obtain the Euclidean form of a vector is to multiply the contravariant vector by the matrix $\text{diag}(i, 1, 1, 1)$ or the covariant vector by $\text{diag}(-i, 1, 1, 1)$ and set $t = -i\tau$. Note that the spatial components do not change. For example, the Euclidean position four-vector, the four-divergence and the zeroth gamma matrix are in terms of their Minkowski definitions Eq. (C3)

$$x_\mu^E = (ix^0, \mathbf{x}) = (-ix_0, \mathbf{x}) = (it, \mathbf{x}) = (\tau, \mathbf{x}),$$

$$\partial_\mu^E = (i\partial^0, \nabla) = (-i\partial_0, \nabla) = \left(-i\frac{\partial}{\partial t}, \nabla\right) = (\partial_\tau, \nabla),$$

$$\gamma_0^E = i\gamma^0 = -i\gamma_0 = \begin{pmatrix} 1 & 0 \\ 0 & -1 \end{pmatrix}.$$

Generalizations to tensors is straightforward and follows for instance from the example $A_{\mu\nu} = a_\mu a_\nu$. Using the above procedure to find the Euclidean versions of all tensors, the partition function is easily found from Eqs. (C1) and (C2) by setting the tensors to their Euclidean versions, taking $\eta_{\mu\nu} \to \delta_{\mu\nu}$ and $t \to -i\tau$. The partition function is

$$Z = \int \mathcal{D}A_\mu \mathcal{D}\bar{\psi}\mathcal{D}\psi\mathcal{D}\bar{\eta}\mathcal{D}\eta\, e^{-S^E},$$

where the Euclidean action is defined as

$$S^E = \int \mathcal{L}_{\text{QCD}}^E d\tau d\mathbf{x},$$

with the Euclidean Lagrangian

$$L_{\text{QCD}}^E = \sum_f [\bar{\psi}_f(\partial + m_f - \gamma_0\mu_f)\psi_f - ig\bar{\psi}_f\gamma_\mu t^a \psi_f A_\mu^a]$$

$$+ \frac{1}{2}A_\mu^a(\partial_\mu\partial_\nu - \partial^2\delta_{\mu\nu})A_\nu^a + \bar{\eta}^a\partial^2\eta^a$$

$$+ gf^{abc}(\bar{\eta}^a\partial_\mu\eta^b)A_\mu^c + \frac{1}{2}g(\partial_\mu A_\nu^a - \partial_\nu A_\mu^a)f^{abc}A_\mu^b A_\nu^c$$

$$+ \frac{1}{4}g^2 f^{abc}f^{ade}A_\mu^b A_\nu^c A_\mu^d A_\nu^e - \frac{1}{2\xi}(\partial_\mu A_\mu^a)^2.$$

In the above the tensors are all Euclidean but the index E has been dropped for convenience, the conjugate fields are now defined as $\bar{\psi}_f = \psi_f^\dagger\gamma_0^E$ and $\bar{\eta} = \eta^\dagger\gamma_0^E$ and the chemical potential has been added as the Lagrange multiplier of the density $\psi_f^\dagger\psi_f$. Additionally, to complete the connection between quantum field theory and statistical field theory, the time integration domain is changed to $\tau \in [0, \beta]$, where β is the inverse temperature T of the system. Because of the definition of the partition function as a trace over all states, the bosonic (fermionic) fields are required to obey symmetric (antisymmetric) boundary conditions, namely $\psi_f(\tau = 0, \mathbf{x}) = \pm\psi_f(\tau = \beta, \mathbf{x})$.

APPENDIX D: NONZERO TEMPERATURE CALCULATIONS

At nonzero temperature, one needs to calculate Matsubara summations which usually can be done using contour integration. In the following, an expression is derived for such summations and the interpretation of the result is discussed. Consider to this end the sum over bosonic Matsubara frequencies ($\omega_n = 2n\pi T$) of the function $f(i\omega_n)$

$$\beta^{-1}\sum_{\omega_n} f(i\omega_n) = \frac{1}{2\pi i} \oint_{C_{\text{mats}}} f(z)\frac{1}{e^{\beta z}-1}dz,$$

where the contour C_{mats} is given in Fig. 10. If $f(z)N_B(z)z \to 0$ when $|z| \to \infty$ then it is possible to close the contour by adding the arcs of $C^{\pm}_{\text{semi-circ}}$, in which case $C_{\text{mats}} = C^{+}_{\text{semi-circ}} + C^{-}_{\text{semi-circ}}$. In general, $f(z)$ will only have poles or branch cuts on the real axis, such that the contours can be contracted along the real axis, which gives

$$\beta^{-1}\sum_{\omega_n} f(i\omega_n) = \frac{1}{\pi} \int_0^\infty N_B(\omega)\Im[f(\omega + i0)]d\omega$$
$$- \frac{1}{\pi} \int_0^\infty [1 + N_B(\omega)]\Im[f(-\omega + i0)]d\omega,$$

$$(D1)$$

where $2i\Im[f(\omega + i0)] \equiv f(\omega + i0) - f(\omega - i0)$ and it was used that $\omega < 0$ for the contour $C^{-}_{\text{semi-arc}}$, such that it is more convenient to take $\omega \to -\omega$ and use $N_B(-\omega) = -1 - N_B(\omega)$. The first line can be interpreted as due to thermal gluons and the second line due to thermal (anti)gluons and a vacuum contribution. The fact that the gluon is its own antiparticle will be reflected by $\Im[f(-\omega + i0)] = -\Im[f(\omega + i0)]$.

Let us evaluate the above for the specific case $f(z) = \ln[g(z)]$ which satisfies $\Im[g(-\omega + i0)] = -\Im[g(\omega + i0)]$. Expanding the logarithm in terms of its real and imaginary parts

$$\ln[g(z)] = \ln|g(z)| + i\arctan\left(\frac{\Im[g(z)]}{\Re[g(z)]}\right)$$
$$+ i\pi\Theta(-\Re[g(z)])\text{sgn}(\Im[g(z)]),$$

then Eq. (D1) can be written as

$$\beta^{-1}\sum_{\omega_n} \ln[g(i\omega_n)] = \frac{1}{\pi} \int_0^\infty d\omega(1 + 2N_B(\omega))$$
$$\times \left[\arctan\left(\frac{\Im[g(\omega_+)]}{\Re[g(\omega_+)]}\right)\right.$$
$$\left. + \pi\Theta(-\Re[g(\omega_+)])\text{sgn}(\Im[g(\omega_+)])\right],$$

which will be used in the calculation of the RPA correction to the thermodynamic potential.

For fermionic Matsubara frequencies a similar derivation can be done, but now the chemical potential is included by writing $f(i\omega_n + \mu)$

$$\beta^{-1}\sum_{\omega_n} f(i\omega_n + \mu) = -\frac{1}{2\pi i} \oint_{C_{\text{mats}}} f(z)\frac{1}{e^{\beta(z-\mu)}+1}dz,$$

where the contour C_{mats} is given in Fig. 11 and $N(z) \equiv (\exp(\beta z) + 1)^{-1}$ has poles at the fermionic Matsubara frequencies with residue -1. If $f(z)N(z)z \to 0$ when $|z| \to \infty$, then it is possible to close the contour as given in Fig. 11 by adding the arcs of $C^{\pm}_{\text{semi-circ}}$ and the lower- and upper-boundaries of C_{box}. The full Matsubara sum can thus be written as a contour integral over $C_{\text{mats}} = C^{+}_{\text{semi-circ}} + C_{\text{box}} + C^{-}_{\text{semi-circ}}$. Again if $f(z)$ only has poles and branch cuts on the real axis, contracting the contours along the real axis gives
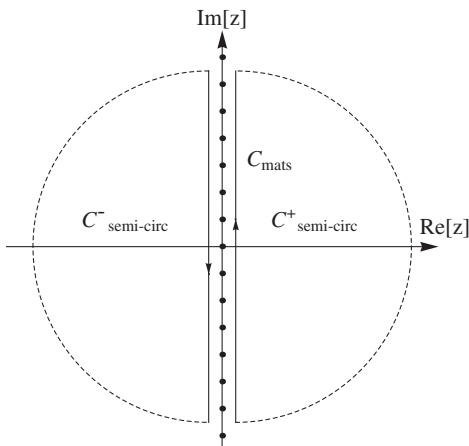

FIG. 10. The contour for the bosonic Matsubara summation, where C_{mats} along the imaginary axis is used to rewrite the frequency summation as a contour integral. The contours $C^{\pm}_{\text{semi-circ}}$ are the positive and negative energy semicircular contours obtained by adding arcs at infinity to C_{mats}.
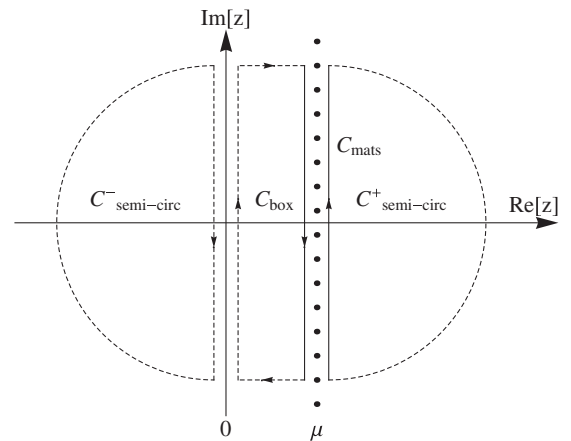

FIG. 11. The same as in Fig. 10 but for the fermionic case, where C_{box}, the contour between $0 < \omega < \mu$, is related to processes inside the Fermi sphere.

$$\beta^{-1}\sum_{\omega_n} f(i\omega_n + \mu) = -\frac{1}{\pi}\int_\mu^\infty N(\omega - \mu)\Im[f(\omega + i0)]d\omega - \frac{1}{\pi}\int_0^\mu [1 - N(\mu - \omega)]\Im[f(\omega + i0)]d\omega$$

$$-\frac{1}{\pi}\int_0^\infty [1 - N(\omega + \mu)]\Im[f(-\omega + i0)]d\omega, \tag{D2}$$

where in the first-to-last line it was used that $0 < \omega < \mu$ for the contour C_{box}, such that it is more convenient to write $N(\omega - \mu) = 1 - N(\mu - \omega)$. Similarly for $C_{\text{semi-circ}}^-$, where $\omega < 0$, we take $\omega \rightarrow -\omega$ in the integral and write $N(-\omega - \mu) = 1 - N(\omega + \mu)$. From the above it is clear that the first line corresponds to particles above the Fermi sphere, the second line to those in the Fermi sphere and the last line is due to antiparticles and contains a vacuum contribution. Note that the above formula must be used with care, since one has to check if the above simplifications are valid on a case-to-case basis.

APPENDIX E: THE GLUON SELF-ENERGY

The gluon self-energy, or the so-called polarization tensor, is given to the lowest order by

$$\Pi_{f,\mu\nu}^{ab} = -g^2 t_{ij}^a t_{ji}^b \int \frac{d^4P}{\mathcal{V}} \text{Tr}_s[\gamma_\mu G_{0f}(P + Q)\gamma_\nu G_{0f}(P)]$$

$$\equiv \delta^{ab}\Pi_{f,\mu\nu}. \tag{E1}$$

The polarization tensor is purely transverse, i.e., $Q_\mu \Pi_{f,\mu\nu} = 0$, which can be easily seen using

$$i\not{Q} = G_{0f}^{-1}(P + Q) - G_{0f}^{-1}(P),$$

and the cyclicity of the trace. Expanding the polarization tensor in terms of the longitudinal and transverse parts relative to the three-momentum $\mathbf{q}$ gives

$$\Pi_{f,\mu\nu} = F_f P_{\mu\nu}^L + G_f P_{\mu\nu}^T,$$

where F_f and G_f can be obtained by

$$F_f = \frac{Q^2}{q^2}\Pi_{f,00}, \qquad G_f = \frac{1}{2}(\Pi_{f,\mu\mu} - F_f). \tag{E2}$$

Noticing that even in the imbalanced case, the contribution from each flavor simply adds up to the total polarization tensor, therefore, throughout this section, we will not explicitly write out the subscript f, and all the formulae presented here are applicable to any flavor. However, in the main text, we use $\Pi_{\mu\nu}$, F and G as the summation over all flavors if the subscript f is not explicitly shown.

After performing the Matsubara sum, the individual processes involved can be identified

$$\Pi_{\mu\nu} = \frac{g^2}{2}\int \frac{d^3p}{(2\pi)^3}\left\{\frac{\sum_{ss'}[\bar{u}_s(\mathbf{p})\gamma_\mu u_{s'}(\mathbf{p}+\mathbf{q})\bar{u}_{s'}(\mathbf{p}+\mathbf{q})\gamma_\nu u_s(\mathbf{p})]}{i\omega_q - \epsilon_0(\mathbf{p}+\mathbf{q}) + \epsilon_0(\mathbf{p})}[N(\mathbf{p}+\mathbf{q})(1 - N(\mathbf{p})) - (1 - N(\mathbf{p}+\mathbf{q}))N(\mathbf{p})]\right.$$

$$+ \frac{\sum_{ss'}[\bar{v}_s(\mathbf{p})\gamma_\mu u_{s'}(\mathbf{p}+\mathbf{q})\bar{u}_{s'}(\mathbf{p}+\mathbf{q})\gamma_\nu v_s(\mathbf{p})]}{i\omega_q - \epsilon_0(\mathbf{p}+\mathbf{q}) - \epsilon_0(\mathbf{p})}[N(\mathbf{p}+\mathbf{q})\bar{N}(\mathbf{p}) - (1 - N(\mathbf{p}+\mathbf{q}))(1 - \bar{N}(\mathbf{p}))]$$

$$+ \frac{\sum_{ss'}[\bar{u}_s(\mathbf{p})\gamma_\mu v_{s'}(\mathbf{p}+\mathbf{q})\bar{v}_{s'}(\mathbf{p}+\mathbf{q})\gamma_\nu u_s(\mathbf{p})]}{i\omega_q + \epsilon_0(\mathbf{p}+\mathbf{q}) + \epsilon_0(\mathbf{p})}[(1 - \bar{N}(\mathbf{p}+\mathbf{q}))(1 - N(\mathbf{p})) - \bar{N}(\mathbf{p}+\mathbf{q})N(\mathbf{p})]$$

$$\left. + \frac{\sum_{ss'}[\bar{v}_s(\mathbf{p})\gamma_\mu v_{s'}(\mathbf{p}+\mathbf{q})\bar{v}_{s'}(\mathbf{p}+\mathbf{q})\gamma_\nu v_s(\mathbf{p})]}{i\omega_q + \epsilon_0(\mathbf{p}+\mathbf{q}) - \epsilon_0(\mathbf{p})}[(1 - \bar{N}(\mathbf{p}+\mathbf{q}))\bar{N}(\mathbf{p}) - \bar{N}(\mathbf{p}+\mathbf{q})(1 - \bar{N}(\mathbf{p}))]\right\}$$

$$= \frac{g^2}{2}\sum_{s_1,s_2=\pm 1}\int \frac{d^3p}{(2\pi)^3}\frac{\text{Tr}[P_E^{s_1}(\mathbf{p})\gamma_0\gamma_\mu P_E^{s_2}(\mathbf{p}+\mathbf{q})\gamma_0\gamma_\nu]}{i\omega_q - s_2\epsilon_0(\mathbf{p}+\mathbf{q}) + s_1\epsilon_0(\mathbf{p})}[N^{s_2}(\mathbf{p}+\mathbf{q})(1 - N^{s_1}(\mathbf{p})) - (1 - N^{s_2}(\mathbf{p}+\mathbf{q}))N^{s_1}(\mathbf{p})], \tag{E3}$$

where $N^s(\mathbf{p}) = \frac{1}{\exp[\beta(s\epsilon_0(\mathbf{p})-\mu)+1]}$, $N^+(\mathbf{p}) = N(\mathbf{p})$ is the Fermi distribution of the corresponding flavor and $\bar{N}(\mathbf{p}) = \frac{1}{\exp[\beta(\epsilon_0(\mathbf{p})+\mu)]+1} = 1 - N^-(\mathbf{p})$ is the Fermi distribution for the corresponding antiparticle. The first line is related to particle-hole creation and annihilation, the second and third line to particle-antiparticle (and hole-antihole) production and annihilation, and the last line to antiparticle-

antiparticlehole creation and annihilation. Note that, as expected, the first line vanishes in the $T, \mu \rightarrow 0$ limit and the last line vanishes in the $T \rightarrow 0$ limit. The second and third line contain infinite vacuum $(T, \mu = 0)$ contributions, which need to be renormalized. The gluon self-energy will be decomposed in terms of a matter part, a renormalized vacuum and an infinite vacuum contribution according to

$$\Pi_{\mu\nu}(Q, T, \mu) = \Pi_{\mu\nu}^{\text{mat}} + \Pi_{\mu\nu}^{\text{ren.vac.}} + \Pi_{\mu\nu}^{\text{inf.vac.}},$$

where the various functions have been defined as

$$\Pi_{\mu\nu}^{\text{mat}} \equiv \Pi_{\mu\nu}(Q, T, \mu) - \frac{P_{\mu\nu}}{3}\Pi_{\lambda\lambda}(Q, 0, 0),$$

$$\Pi_{\mu\nu}^{\text{ren.vac.}} \equiv \frac{P_{\mu\nu}}{3}\left[\Pi_{\lambda\lambda}(Q, 0, 0) - Q^2\left(\frac{\Pi_{\lambda\lambda}(Q, 0, 0)}{Q^2}\right)_{Q^2\to 0}\right],$$

$$\Pi_{\mu\nu}^{\text{inf.vac.}} \equiv \frac{P_{\mu\nu}}{3}Q^2\left[\frac{\Pi_{\lambda\lambda}(Q, 0, 0)}{Q^2}\right]_{Q^2\to 0}.$$

For the vacuum expressions, it is possible to extract the projection matrix $P_{\mu\nu}$, since the polarization tensor is purely transverse and for $T, \mu = 0$ there is no preferential frame such that the tensor is built up out of only two possible quantities $\delta_{\mu\nu}$ and $Q_\mu Q_\nu$. To include the dynamical properties of the vacuum expression a renormalization procedure is necessary. In the above the renormalized

vacuum expression was obtained by extracting the infinite contributions from the vacuum polarization tensor at the renormalization point $Q^2 = 0$. The reason for extracting the factor Q^2 from the vacuum $\Pi_{\lambda\lambda}$ before setting $Q^2 = 0$ is because in the vacuum the dressed gluons are massless, i.e., $\Pi_{\lambda\lambda} \propto Q^2$, c.f. Eq. (E7). Therefore, $Q^2 = 0$ is still a pole for the vacuum expression, at which the residue is 1 after the renormalization. In conclusion, the following full renormalized polarization tensor will be used:

$$\Pi_{\mu\nu}^{\text{ren}} = \Pi_{\mu\nu} - \Pi_{\mu\nu}^{\text{inf.vac.}} = \Pi_{\mu\nu}^{\text{mat}} + \Pi_{\mu\nu}^{\text{ren.vac.}}. \tag{E4}$$

In the high-density limit ($\mu \gg m$), a good approximation is to evaluate the matter part for the case of massless quarks. Thus for massless quarks in the zero-temperature limit the matter parts of Π_{00} and $\Pi_{\mu\mu}$ can be calculated explicitly

$$\Pi_{00}^{\text{mat}}(T = 0) = \frac{g^2}{2\pi^2}\left\{\frac{2}{3}\mu^2 - \frac{1}{24}\sum_{s_1, s_2 = \pm 1}\left[q^2 - \frac{is_1\omega_q}{2q}(Q^2 + 2q^2)\right]\ln\left[1 - \frac{2s_1 s_2\mu}{q - is_1\omega_q}\right]\right.$$

$$\left. + \sum_{s_2 = \pm 1}\left[s_2\frac{\mu(3Q^2 - 4\mu^2)}{24q} - \frac{\mu^2}{4}\frac{i\omega_q}{q}\right]\ln\left[\frac{1 - \frac{2s_2\mu}{q - i\omega_q}}{1 + \frac{2s_2\mu}{q + i\omega_q}}\right]\right\}, \tag{E5}$$

$$\Pi_{\mu\mu}^{\text{mat}}(T = 0) = \frac{g^2}{\pi^2}\left[\frac{\mu^2}{2} - \frac{Q^2}{8q}\left\{\mu\sum_{s_1 = \pm 1}s_1\ln\left[\frac{1 + \frac{2s_1\mu}{q - i\omega_q}}{1 - \frac{2s_1\mu}{q + i\omega_q}}\right] + \frac{1}{2}\sum_{s_1, s_2 = \pm 1}(q - is_1\omega_q)\ln\left[1 + \frac{2s_1 s_2\mu}{q - is_1\omega_q}\right]\right\}\right]. \tag{E6}$$

These expressions give the same result as can be found in Refs. [41–43]. Performing an analytic continuation to real time ($i\omega_q \to \omega + i0$), the above expressions have branch cuts from $\max(0, q - 2\mu) < |\omega| < q$ and $q < |\omega| < q + 2\mu$, the origins of which can be found from Eq. (E3) and are due to particle-hole processes and finite-T, μ contributions to particle-antiparticle production and annihilation, respectively. Because Lorentz invariance is broken due to

the presence of the gas, Π^{mat} is a function of $q_0 = i(i\omega_q)$ and q separately since it can be a function of $q_\mu u_\mu$ and $q = \sqrt{Q^2 - (q_\mu u_\mu)^2}$, where $u_\mu = (1, 0, 0, 0)$ defines the rest frame of the system [14].

The renormalized vacuum part $\Pi_{\mu\nu}^{\text{ren.vac.}}$ has been found in Ref. [44]

$$P_{\mu\nu}Q^2\frac{g^2}{4\pi^2}\int_0^1 dx\, x(1 - x)\ln\left(\frac{m^2}{m^2 + x(1 - x)Q^2}\right) = -\frac{1}{3}P_{\mu\nu}Q^2\frac{g^2}{4\pi^2}\left[\frac{1}{6} - \left(1 - \frac{2m^2}{Q^2}\right)\left(1 - \sqrt{1 + \frac{4m^2}{Q^2}}\,\text{ArcCoth}\sqrt{1 + \frac{4m^2}{Q^2}}\right)\right]$$

$$\simeq P_{\mu\nu}\frac{g^2 Q^2[\frac{5}{3} + \ln(\frac{m^2}{Q^2})]}{24\pi^2}, \tag{E7}$$

where it was assumed that the quarks have equal masses and in the last line it was expanded for small masses. In real time, this expression has a branch cut for $|\omega| > \sqrt{q^2 + 4m^2} \simeq q$, which is due to particle-antiparticle production and annihilation.

Using a Sommerfeld expansion temperature, corrections to the gluon self-energy can be obtained. The Sommerfeld expansion can be summarized as

$$N(\epsilon_p - \mu) = \Theta(\mu - \epsilon_p) - \sum_{n=1}^{\infty} 2(1 - 2^{1-2n})\zeta(2n)\frac{\partial^{2n-1}}{\partial\epsilon_p^{2n-1}}\delta(\epsilon_p - \mu)T^{2n}. \tag{E8}$$

The derivation is analogous to that of the nonrelativistic Sommerfeld expansion [45]. One has to keep in mind that the above is not a complete expansion for small temperatures since also the chemical potential depends on temperature. In this manner the T^2 correction to the gluon self-energy is found to be

$$\Pi_{00}^{\text{mat}} - \Pi_{00}^{\text{mat}}(T=0) = \frac{g^2}{2}\frac{1}{6}T^2 \sum_{s=\pm 1} \frac{i\omega_q + 2s\mu}{2q} \ln\left[\frac{(i\omega_q - q)(i\omega_q + 2s\mu + q)}{(i\omega_q + q)(i\omega_q + 2s\mu - q)}\right],$$

$$\Pi_{\mu\mu}^{\text{mat}} - \Pi_{\mu\mu}^{\text{mat}}(T=0) = -\frac{g^2}{2}\frac{1}{6}T^2 \frac{8\mu^2[3(i\omega_q)^2 - (2\mu - q)(2\mu + q)]}{[(i\omega_q)^2 - (2\mu - q)^2][(i\omega_q)^2 - (2\mu + q)^2]}. \tag{E9}$$

Using Eqs. (E2)–(E4) and (E6)–(E9) the behavior of F and G can be found in several limits. Keeping the ratio $x = q/\omega$ fixed and expanding up to zeroth order in ω, the hard dense loop and hard thermal loop (HDL/HTL) expressions are reobtained [13,14]

$$\lim_{\omega\to 0} F(\omega, q = x\omega) = 2m_g^2\left(1 - \frac{1}{x^2}\right)\left[1 + \frac{1}{2x}\ln\left(\frac{1-x}{1+x}\right)\right]\Big|_{x=q/\omega},$$

$$\lim_{\omega\to 0} G(\omega, q = x\omega) = m_g^2\left[\frac{1}{x^2} - \frac{1}{2x}\left(1 - \frac{1}{x^2}\right)\ln\left(\frac{1-x}{1+x}\right)\right]\Big|_{x=q/\omega}, \quad \text{where } m_g^2 \equiv \frac{g^2}{4\pi^2}\left(\mu^2 + \frac{1}{3}\pi^2 T^2\right), \tag{E10}$$

is the gluon thermal mass. The reason that the above limit returns the HDL and HTL expressions, is due to the fact that the HDL/HTL approximation ($m = 0$ and $\omega \ll q \ll \mu$) takes into account only the low-energy processes around the Fermi surface, namely, particle-hole processes. Some other useful limits are

$$\lim_{q\to 0}\lim_{\omega\to 0} F = 2m_g^2\left(1 + i\frac{\pi}{2}\frac{\omega}{q}\right),$$

$$\lim_{q\to 0}\lim_{\omega\to 0} G = -2m_g^2 i\frac{\pi}{2}\frac{\omega}{q},$$

where it can be seen that in the static long-wavelength limit ($\omega, q \to 0$) the electric gluons (F) are screened, while magnetic gluons (G) are dynamically screened. Furthermore, the large momenta and frequency behavior of the matter and vacuum parts are separately seen to be

$$\lim_{q,\omega\to\infty} F^{\text{mat}} = \frac{\mu^2(4m_g^2 + \frac{5}{3}g^2 T^2)}{3Q^2},$$

$$\lim_{q,\omega\to\infty} G^{\text{mat}} = -\frac{\mu^2(4m_g^2 + \frac{5}{3}g^2 T^2)(q^2 + \omega^2)}{3Q^4}, \tag{E11}$$

$$\lim_{\substack{q,\omega\to\infty \\ T,\mu\to 0}} F, G = \frac{g^2 Q^2[\frac{5}{3} + \ln(\frac{m^2}{Q^2})]}{24\pi^2}.$$

The vacuum expressions are proportional to Q^2 since in the vacuum the gluons remain massless and thus $Q^2 = 0$ is still a pole of the propagator. The logarithmic Q^2 dependence is usually absorbed into the vertex and subsequently interpreted as the varying of the coupling constant with the energy scale Q.

APPENDIX F: THE THERMODYNAMIC POTENTIAL OF IDEAL GASES

Consider first the well-known ideal Fermi gas term of a single species

$$-\frac{1}{V\beta}\text{Tr}\ln(-G_0^{-1})$$

$$= -\frac{1}{V\beta}\sum_{\omega_n,p}\text{lndet}[(i\not{p} + m)]$$

$$= -\frac{1}{\beta}\sum_{\omega_n}\int\frac{d^3p}{(2\pi)^3}2\ln[-(i\omega_n + \mu_0)^2 + \epsilon_0^2(\mathbf{p})].$$

Using Eq. (D2) with $f(z) = \ln[-z^2 + \epsilon_0^2(\mathbf{p})]$ and using the principle value logarithm with a branch cut on the negative real axis

$$\lim_{\eta\downarrow 0}\Im[f(\omega + i\eta)] = \lim_{\eta\downarrow 0}\Im[\ln(-\omega^2 + \epsilon_0^2(\mathbf{p}) - 2i\omega\eta)]$$

$$= \pi\Theta[\omega^2 - \epsilon_0^2(\mathbf{p})]\text{sgn}(-\omega),$$

the ideal Fermi gas contribution becomes

$$-2\int\frac{d^3p}{(2\pi)^3}\int_0^{\infty}[N(\omega - \mu_0) - (1 - N(\omega + \mu_0))]$$

$$\times \Theta[\omega^2 - \epsilon_0^2(\mathbf{p})]d\omega$$

$$= -2\beta^{-1}\int\frac{d^3p}{(2\pi)^3}\{\ln[1 + e^{-\beta(\epsilon_0(\mathbf{p}) - \mu_0)}]$$

$$+ \ln[1 + e^{-\beta(\epsilon_0(\mathbf{p}) + \mu_0)}]\} + 2\int\frac{d^3p}{(2\pi)^3}\int_{\epsilon_0^2(\mathbf{p})}^{\infty}d\omega.$$

In the above it was assumed that the arc at infinity vanishes, which is the case if the time-ordering in the path-integral is

taken into account properly by multiplying the integrand by $e^{-i\omega_n \eta}$ and taking the limit $\eta \downarrow 0$. The infinite vacuum contribution is clearly visible and should be subtracted, giving for massless fermions

$$\Omega_{\text{ideal-Fermi}} = -\left[\frac{7\pi^2 T^4}{180} + \frac{T^2 \mu_0^2}{6} + \frac{\mu_0^4}{12\pi^2}\right].$$

The ideal Bose gas follows from

$$\frac{1}{V\beta} \frac{1}{2} \text{Tr}\left[\ln(D_0^{-1}) - 2\ln(\partial_\mu f_\mu) - \ln\frac{1}{\xi}\right],$$

which will lead to the same expression in both the Lorentz and Coulomb gauges. In the following, the Coulomb gauge is taken ($f_\mu = (0, \nabla)_\mu$),

$$\frac{1}{2V\beta}\left(\text{Tr}\ln[D_{0,\mu\nu}^{-1}(Q)] - 2\,\text{Tr}\ln q^2 - \text{Tr}\ln\frac{1}{\xi}\right)$$

$$= \frac{1}{2V\beta}\sum_{\omega_n, q}\left(\ln\left[\frac{q^2}{\xi}q^2(Q^2)^2\right] - 2\ln q^2 - \ln\frac{1}{\xi}\right)$$

$$= \frac{1}{V\beta}\sum_{\omega_n, q}\ln[-(i\omega_n)^2 + q^2].$$

The unphysical degrees of freedom clearly drop out due to the ghost contribution $\partial_\mu f_\mu$. Using Eq. (D1) with $f(z) = \ln(-z^2 + q^2)$, the ideal Bose gas contribution is

$$\frac{2}{\beta}\int\frac{d^3q}{(2\pi)^3}\ln[1 - e^{-\beta q}] - \int\frac{d^3q}{(2\pi)^3}\int_q^\infty d\omega.$$

Again, the vacuum term is clearly present and will be subtracted, giving the Stefan-Boltzmann law

$$\Omega_{\text{ideal-Bose}} = -\frac{T^4}{45\pi^2}.$$

APPENDIX G: THE QUARK SELF-ENERGY

For completeness also, the quark self-energy will be derived in the Lorentz gauge to lowest order.

$$\Sigma(P) = \int\frac{d^4Q}{V}\text{Tr}[-ig\gamma_\mu t^a G_0(Q)(-ig\gamma_\nu t^a)D_{\mu\nu}(P - Q)].$$

Performing the Matsubara sum gives

$$\Sigma(i\omega_p, \mathbf{p}) = -g^2\frac{N_G}{2N_C}\int\frac{d^3q}{(2\pi)^3}\frac{1}{2\epsilon^g(\mathbf{p} - \mathbf{q})}\left\{\frac{\sum_s[\gamma_\mu u_s(\mathbf{q})\bar{u}_s(\mathbf{q})\gamma_\mu]}{i\omega_p + \mu - \epsilon_0(\mathbf{q}) - \epsilon^g(\mathbf{p} - \mathbf{q})}[(1 + N_B(\mathbf{p} - \mathbf{q}))(1 - N(\mathbf{q}))\right.$$

$$+ N_B(\mathbf{p} - \mathbf{q})N(\mathbf{q})] + \frac{\sum_s[\gamma_\mu u_s(\mathbf{q})\bar{u}_s(\mathbf{q})\gamma_\mu]}{i\omega_p + \mu - \epsilon_0(\mathbf{q}) + \epsilon^g(\mathbf{p} - \mathbf{q})}[N_B(\mathbf{p} - \mathbf{q})(1 - N(\mathbf{q})) + (1 + N_B(\mathbf{p} - \mathbf{q}))N(\mathbf{q})]$$

$$+ \frac{\sum_s[\gamma_\mu v_s(\mathbf{q})\bar{v}_s(\mathbf{q})\gamma_\mu]}{i\omega_p + \mu + \epsilon_0(\mathbf{q}) - \epsilon^g(\mathbf{p} - \mathbf{q})}[(1 + N_B(\mathbf{p} - \mathbf{q}))\bar{N}(\mathbf{q}) + N_B(\mathbf{p} - \mathbf{q})(1 - \bar{N}(\mathbf{q}))]$$

$$\left.+ \frac{\sum_s[\gamma_\mu v_s(\mathbf{q})\bar{v}_s(\mathbf{q})\gamma_\mu]}{i\omega_p + \mu + \epsilon_0(\mathbf{q}) + \epsilon^g(\mathbf{p} - \mathbf{q})}[N_B(\mathbf{p} - \mathbf{q})\bar{N}(\mathbf{q}) + (1 + N_B(\mathbf{p} - \mathbf{q}))(1 - \bar{N}(\mathbf{q}))]\right\},$$

$$\Delta\Sigma(i\omega_p, \mathbf{p}) = -g^2\frac{N_G}{4N_C}\sum_{s_2, s_3 = \pm 1}\int\frac{d^3q}{(2\pi)^3}\left[\frac{s_3}{\epsilon^g(\mathbf{p} - \mathbf{q})}\frac{\gamma_\mu P_E^{s_2}(\mathbf{q})\gamma_0\gamma_\mu}{i\omega_p + \mu - s_2\epsilon_0(\mathbf{q}) - s_3\epsilon^g(\mathbf{p} - \mathbf{q})}\right]$$

$$\times [(1 + N_B^{s_3}(\mathbf{p} - \mathbf{q}))(1 - N^{s_2}(\mathbf{q})) + N_B^{s_3}(\mathbf{p} - \mathbf{q})N^{s_2}(\mathbf{q}) - I_{s_2, s_3}]. \tag{G1}$$

In the last line the indicator function $I_{s_2, s_3} = \delta_{s_2+}\delta_{s_3+} - \delta_{s_2-}\delta_{s_3-}$ is exactly the vacuum contribution such that $\Delta\Sigma$ is the vacuum subtracted self-energy, i.e., $\Delta\Sigma(T = \mu = 0) = 0$. To first order, the self-energy for a single quark and antiquark can be found by using the free quark energy projectors and helicity projectors

$$\Sigma_s^{s_1}(i\omega_p, \mathbf{p}) = \text{Tr}[\mathcal{P}^s(\mathbf{p})P_E^{s_1}\gamma_0\Sigma(i\omega_p, \mathbf{p})].$$

After projecting and evaluating the self-energy at $i\omega_p = s_1\epsilon_0(\mathbf{p}) - \mu$, the function in the first square brackets in Eq. (G1) reduces to $\mathcal{F}_{s_1, s_2, s_3}(\mathbf{p}, \mathbf{q})$ defined in Eq. (14). In the zero-temperature limit the self-energy for a single quark then reduces to

$$\lim_{T \to 0}\Delta\Sigma^+(\epsilon_0(\mathbf{p}) - \mu, \mathbf{p}) = \frac{g^2 N_G}{4N_C}\sum_{s_3 = \pm 1}\int\frac{d^3q}{(2\pi)^3}\mathcal{F}_{+, +, s_3}(\mathbf{p}, \mathbf{q})N^+(\mathbf{q}). \tag{G2}$$

Note that the final result is independent of helicity s.

[1] P. Nozieres, *Theory of Interacting Fermi Systems* (Westview, Boulder, 1997).

[2] J. W. Negele and H. Orland, *Quantum Many-Particle Systems* (Westview, Boulder, 1998).

[3] G. Baym and C. Pethick, *Landau Fermi-Liquid Theory: Concepts and Applications* (Wiley-VCH, New York, 2004).

[4] G. D. Mahan, *Many Particle Physics* (Springer, New York, 2000).

[5] A. J. Leggett, Rev. Mod. Phys. **71**, S318 (1999).

[6] J. R. Schrieffer and M. Tinkham, Rev. Mod. Phys. **71**, S313 (1999).

[7] M. G. Alford, A. Schmitt, K. Rajagopal, and T. Schäfer, Rev. Mod. Phys. **80**, 1455 (2008).

[8] D. Bailin and A. Love, Phys. Rep. **107**, 325 (1984).

[9] W. Becker, *Neutron Stars and Pulsars* (Springer, New York, 2008).

[10] P. Haensel, A. Y. Potekhin, and D. G. Yakovlev, *Neutron Stars 1: Equation of State and Structure* (Springer, New York, 2006).

[11] *Superdense QCD Matter and Compact Stars: Proceedings of the NATO Advanced Research Workshop on Superdense QCD Matter and Compact Stars*, edited by D. Blaschke and D. Sedrakian (Springer, New York, 2006).

[12] A. J. Leggett, Rev. Mod. Phys. **47**, 331 (1975).

[13] M. Le Bellac, *Thermal Field Theory* (Cambridge University Press, Cambridge, 1996).

[14] J. I. Kapusta and C. Gale, *Finite-Temperature Field Theory: Principles and Applications* (Cambridge University Press, New York, 2006).

[15] D. T. Son, Phys. Rev. D **59**, 094019 (1999).

[16] R. D. Pisarski and D. H. Rischke, Phys. Rev. D **61**, 051501 (2000).

[17] D. K. Hong, V. A. Miransky, I. A. Shovkovy, and L. C. R. Wijewardhana, Phys. Rev. D **61**, 056001 (2000).

[18] C. Manuel, Phys. Rev. D **62**, 076009 (2000).

[19] M. Le Bellac and C. Manuel, Phys. Rev. D **55**, 3215 (1997).

[20] T. Schäfer and K. Schwenzer, Phys. Rev. D **70**, 054007 (2004).

[21] W. E. Brown, J. T. Liu, and H. C. Ren, Phys. Rev. D **62**, 054013 (2000).

[22] M. W. Zwierlein, A. Schirotzek, C. H. Schunck, and W. Ketterle, Science **311**, 492 (2006).

[23] G. B. Partridge, W. Li, R. I. Kamar, Y. Liao, R. G. Hulet, Science **311**, 503 (2006).

[24] R. Casalbuoni and G. Nardulli, Rev. Mod. Phys. **76**, 263 (2004).

[25] P. F. Bedaque, H. Caldas, and G. Rupak, Phys. Rev. Lett. **91**, 247002 (2003).

[26] T. Rice, Ann. Phys. (N.Y.) **31**, 100 (1965).

[27] G. Baym and S. A. Chin, Nucl. Phys. **A262**, 527 (1976).

[28] Because of the inclusion of a small T-correction the spectral functions will no longer satisfy $\rho^{T,L} > 0$.

[29] L. H. Ryder, *Quantum Field Theory* (Cambridge University Press, Cambridge, 1996).

[30] A. Ipp, A. Gerhold, and A. Rebhan, Phys. Rev. D **69**, 011901 (2004).

[31] L. D. Landau and E. M. Lifshitz, *Statistical Physics, Part 1* (Butterworth-Heinemann, Oxford, 1980).

[32] T. Holstein, R. E. Norton, and P. Pincus, Phys. Rev. B **8**, 2649 (1973).

[33] S. Chakravarty, R. E. Norton, and O. F. Syljuaasen, Phys. Rev. Lett. **74**, 1423 (1995).

[34] A. Ipp, K. Kajantie, A. Rebhan, and A. Vuorinen, Phys. Rev. D **74**, 045016 (2006).

[35] A. Gerhold, A. Ipp, and A. Rebhan, Phys. Rev. D **70**, 105015 (2004).

[36] A. Ipp, A. Rebhan, and A. Vuorinen, Phys. Rev. D **69**, 077901 (2004).

[37] A. Ipp and A. Rebhan, J. High Energy Phys. 06 (2003) 032.

[38] D. Boyanovsky and H. J. de Vega, Phys. Rev. D **63**, 034016 (2001).

[39] R. C. Tolman, *Thermodynamics and Cosmology* (Dover, New York, 1987).

[40] L. D. Landau and E. M. Lifshitz, *The Classical Theory of Fields* (Butterworth-Heinemann, Oxford, 1980).

[41] T. Toimela, Int. J. Theor. Phys. **24**, 901 (1985).

[42] J. I. Kapusta, Phys. Rev. D **20**, 989 (1979).

[43] A. Kurkela, P. Romatschke, and A. Vuorinen, Phys. Rev. D **81**, 105021 (2010).

[44] M. E. Peskin and D. V. Schroeder, *An Introduction to Quantum Field Theory* (Westview, Boulder, 1995).

[45] J. Sólyom, *Fundamentals of the Physics of Solids* (Springer, New York, 2008), Vol. 2.